

# Binary-compact-stars, gravitational waves and equation of state

Luca Baiotti

梅乙亭 瑠嘉

Osaka University

# Plan of the talk

- Introduction: basic ideas and state-of-the-art of BNS merger simulations
- Studies of estimates (before the detection)
  - pre-merger
  - post-merger
- Semi-raw information from GW170817
- Constraints imposed by GW170817
  - pre merger (GWs)
  - post merger (ejecta)
  - constrains on the parameters of favourite EoS or favourite assumptions on (methods to compute) EoS
- Conclusions and a summary of estimates

# Basic ideas

- Terrestrial experiments, e.g. neutron-skin thickness, constrain the EoS in various ways and to various degrees up to around nuclear density
- Astrophysical observation (pulsars, X-ray binaries) before GW170817 already gave additional constraints (radius) on the EoS of ultra-high density matter
- Further information on the EoS (constraints of EoS parameters, if an EoS family is allowed at all) of ultra-high density matter can be obtained through BNS mergers observations by determining the
  - Maximum mass of a non-rotating compact star, lest it collapses to a black hole
  - Tidal deformability or radius for a given mass

# Basic ideas

- Observational constraints on the maximum mass of a compact star and its tidal deformability or radius for a given mass can be obtained from BNS mergers through
  - GWs from the late inspiral
  - GWs from post-merger oscillations
  - Nature of the merged object (BH, stable/metastable compact star)
  - Electromagnetic emissions (macronovae)

# State of the art of BNS simulations and the physics they aim to

For work done just before GW170817, see also:

Baiotti and Rezzolla

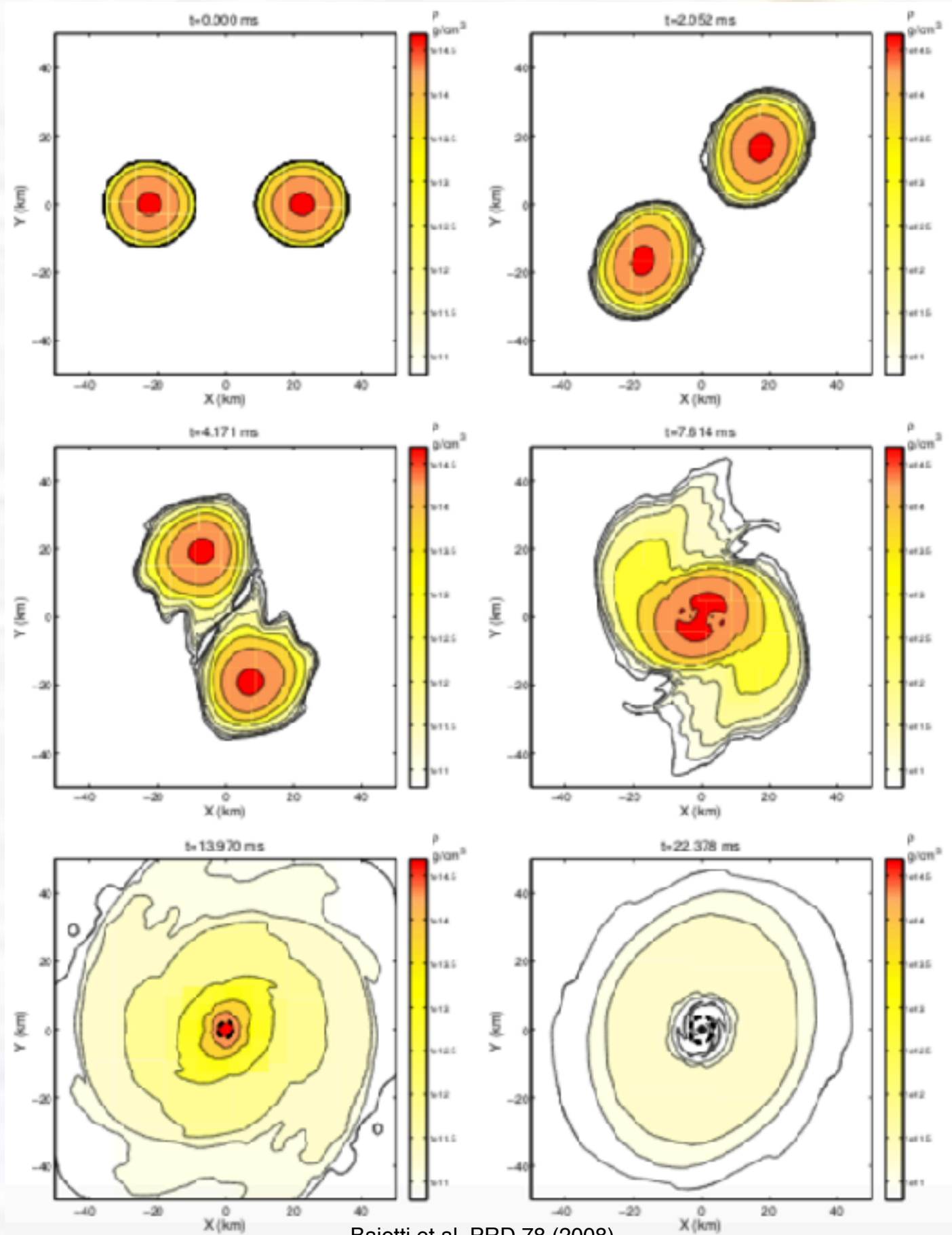
“Binary neutron-star mergers: a review of Einstein's richest laboratory”

[Reports on Progress of Physics 80, 096901 \(2017\)](#)

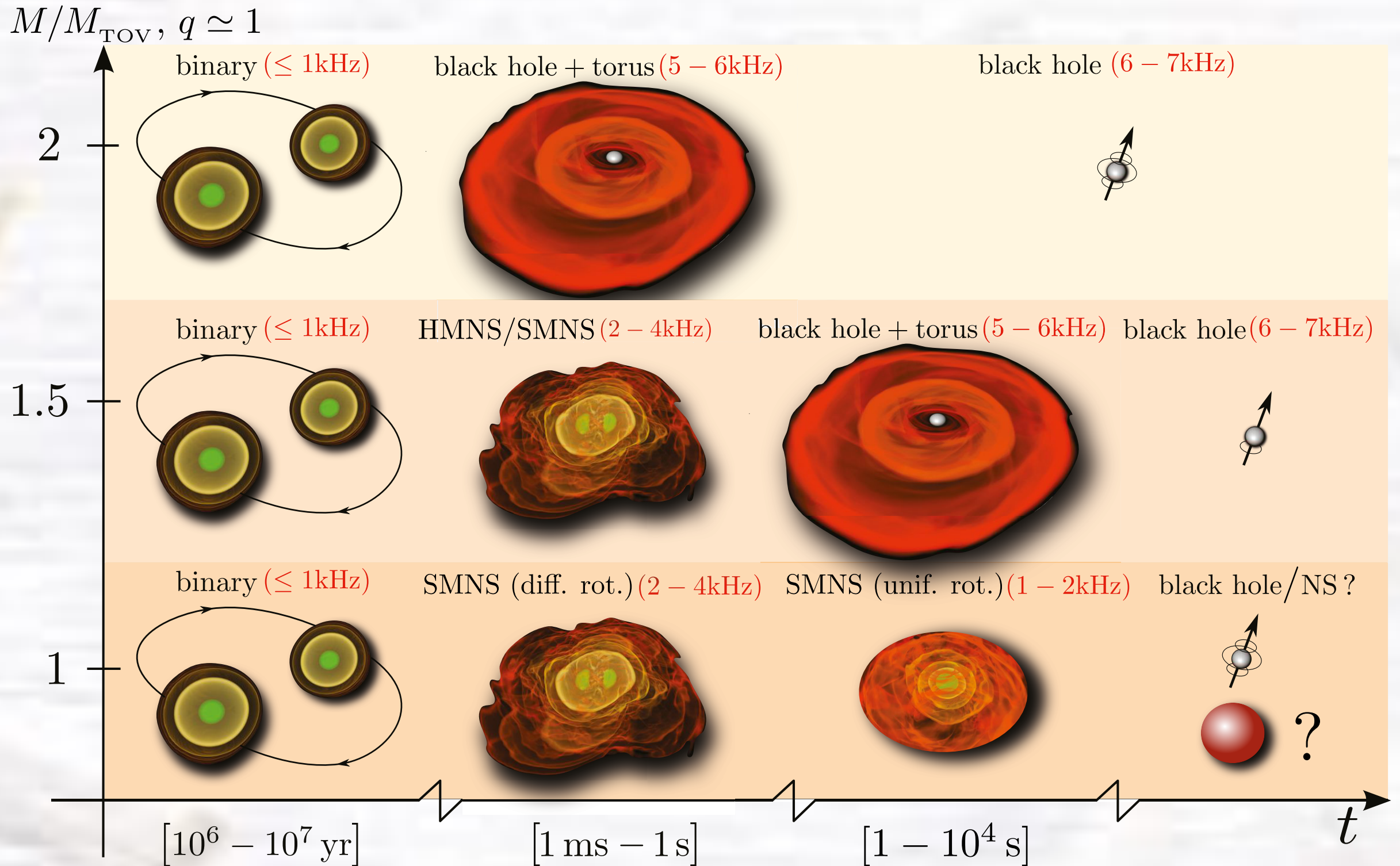
arXiv 1607.03540

DOI: 10.1088/1361-6633/aa67bb

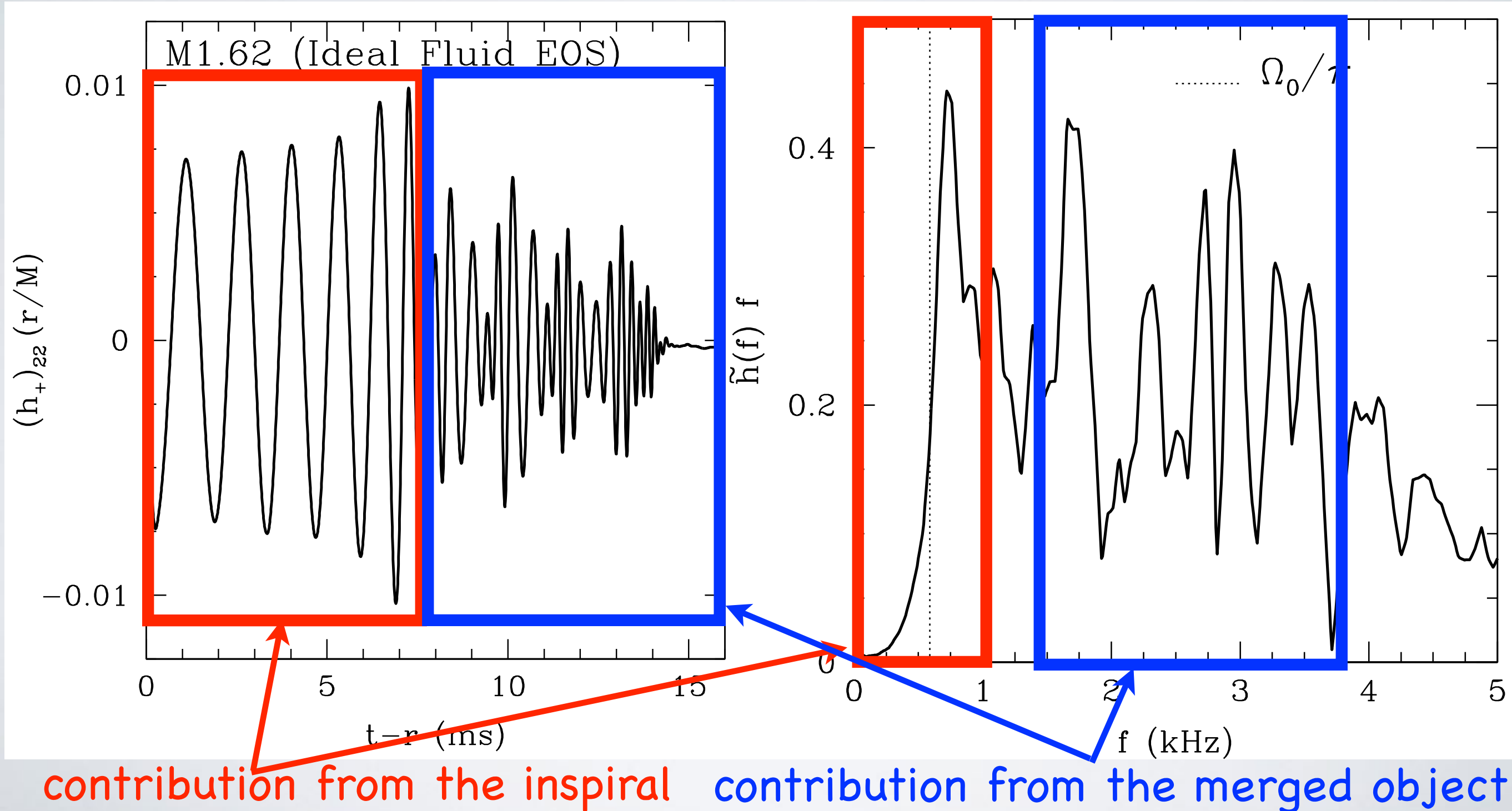
# Dynamics of BNS



# Dynamics of BNS



# GRAVITATIONAL WAVES FROM BINARY NEUTRON STARS



# Numerical relativity

In order to help and interpret observation, we need solutions of the general relativistic equations.

Numerical relativity is the science of simulating (solving) general-relativistic dynamics on computers.

Straightforward discretisation of the Einstein equations are impossible, because:

- formulation is not self-evident: e.g. time is not “simply” defined
- physical singularities may be present
- grid stretching develops
- numerical instabilities are present
- gauges play an important role

# Modelling and simulations of BNS

A few groups are actively working on BNS simulations with their own independent general-relativistic codes

We aim at simulations that include

- Einstein equations and relativistic hydrodynamic equations
- (resistive) magnetohydrodynamics (MHD)
- equations of state based on microphysical calculations
- (neutrino) radiation transport
- nuclear-reaction networks
- high-order, high-accuracy numerical methods
- ...

and is fast enough to allow parameter-space exploration!

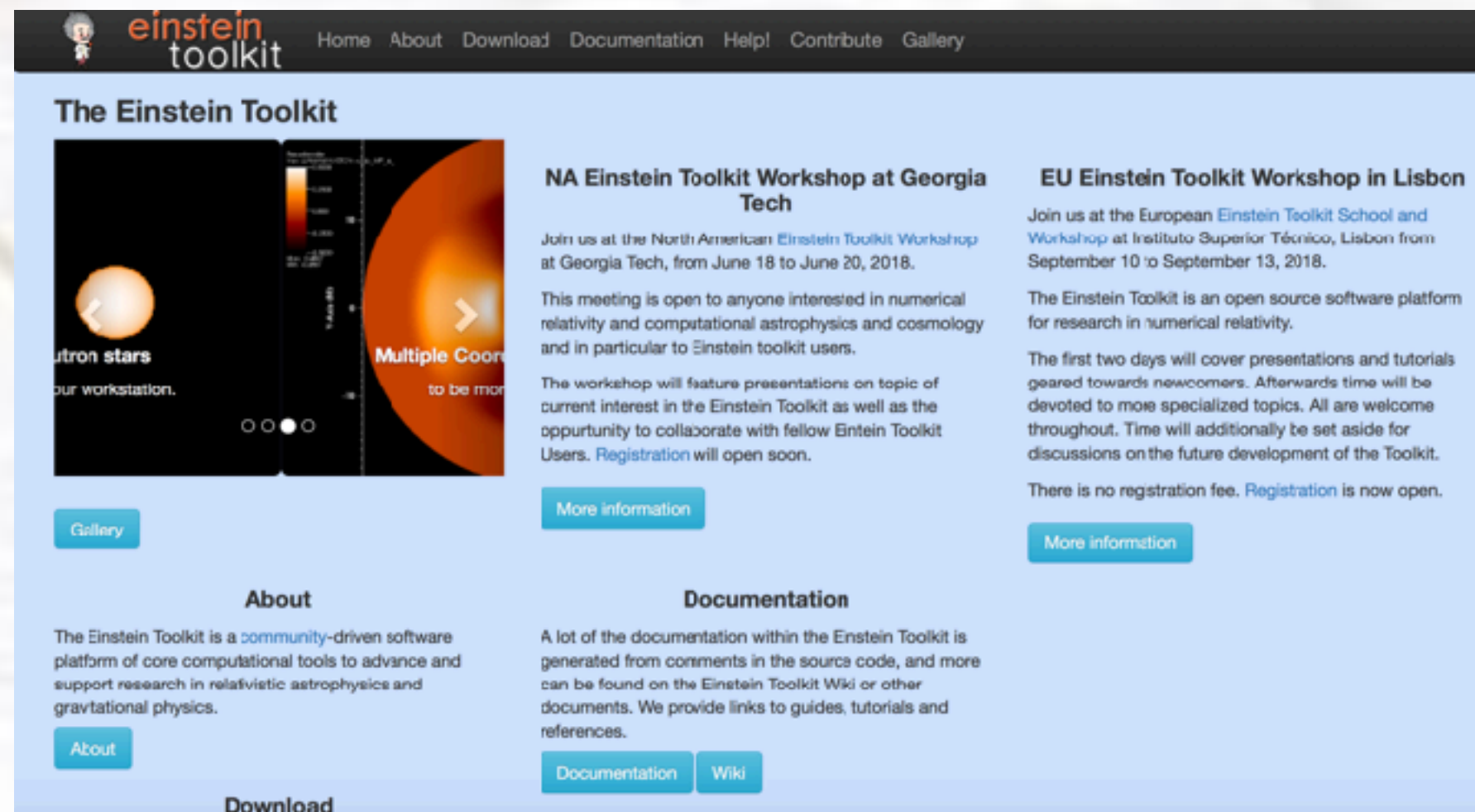
# The Einstein Toolkit

Many codes for numerical relativity are publicly available in the **Einstein Toolkit**, which aims at providing computational tools for the community.

It includes:

- spacetime evolution code
- GRHydro code
- GRMHD codes
- initial-data codes
- mesh refinement
- portability
- simulation management tools

[einsteintoolkit.org](http://einsteintoolkit.org)



The screenshot shows the homepage of the Einstein Toolkit website. The header features the logo and navigation links: Home, About, Download, Documentation, Help, Contribute, and Gallery. The main content area is divided into several sections:

- The Einstein Toolkit**: A central banner with a dark background and orange highlights, featuring a neutron star and a multiple coordinate system visualization. Below it is a "Gallery" button.
- NA Einstein Toolkit Workshop at Georgia Tech**: A section with a teal background containing text about the workshop dates (June 18-20, 2018) and a "More information" button.
- EU Einstein Toolkit Workshop in Lisbon**: A section with a teal background containing text about the workshop dates (September 10-13, 2018) and a "More information" button.
- About**: A section with a teal background containing a brief description of the toolkit and an "About" button.
- Documentation**: A section with a teal background containing text about the documentation and "Documentation" and "Wiki" buttons.

At the bottom of the page, there is a "Download" button.

# Status of modelling and simulations of BNS

## ★ **Robust capabilities** (but improvements are being constantly made):

- ★ matter and spacetime dynamics (including long-term evolutions of the formed BHs and accretion discs); EoS in simulations are either piecewise polytropes (plus a thermal part) or tabulated
- ★ extraction of gravitational-wave signals from the dynamics

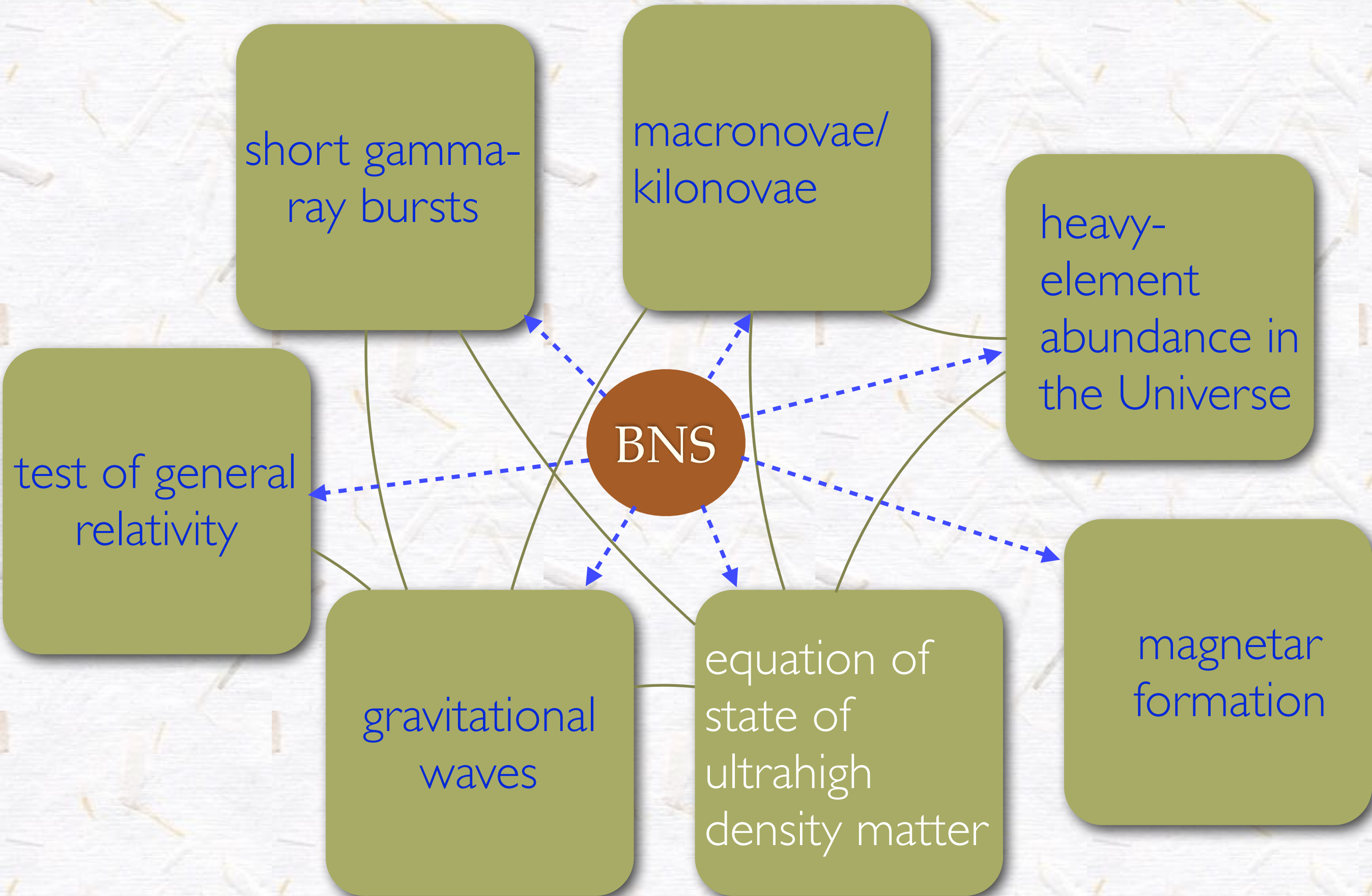
## ★ **Ongoing work on:**

- ★ linking GW observations to physical properties of the emitting system (in particular the EoS)
- ★ heavy-element production and macronovae / kilonovae
- ★ improved initial data (spins, eccentricity)

## ★ **Open issues:**

- ★ magnetic fields after the merger [and before the merger in case of resistive MHD (pre-merger electromagnetic emission)]
- ★ effects of neutrino and photon radiation transport
- ★ (viscosity)

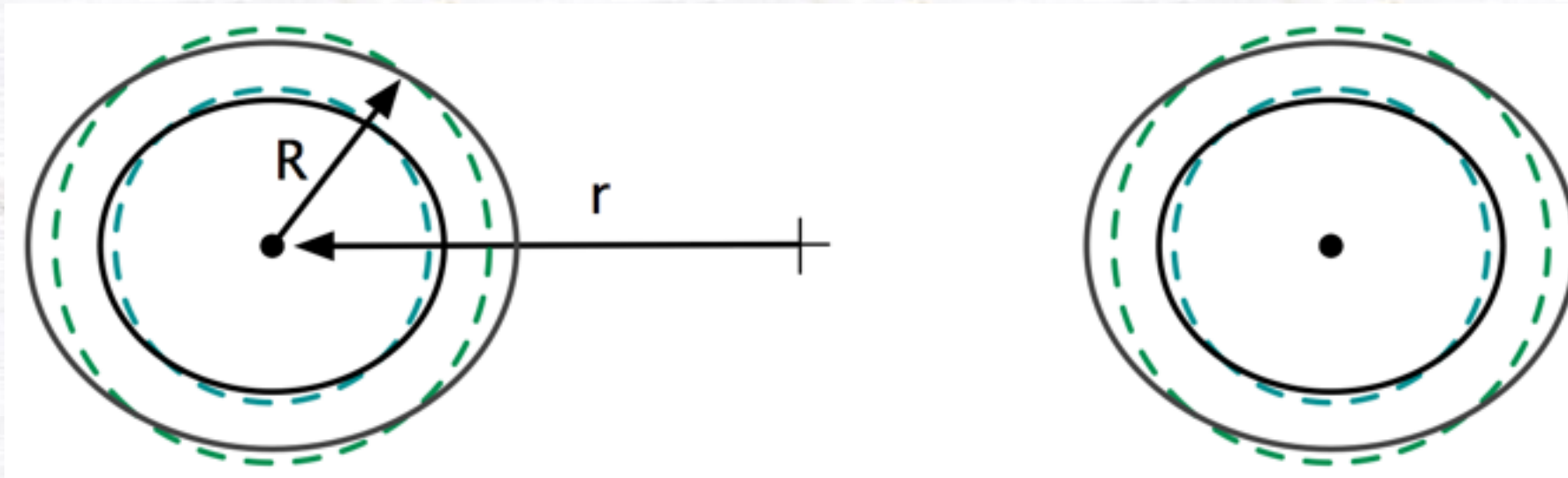
# Interest in binary neutron-star mergers



Studying the compact-star EoS through  
gravitational waves from BNS systems  
**before the merger**

# Tidal deformations

Stars undergo tidal deformations as they get closer.



Tidal deformations are described through the tidal deformability coefficient defined as the proportionality constant between the external tidal field and the quadrupole moment of the star:

$$Q_{ij} = -\lambda E_{ij}$$

Actually tidal deformations are better described through the dimensionless quadrupole deformability:

$$\Lambda = \frac{c^{10}}{G^4 M^5} \lambda \quad \text{also written as} \quad \Lambda = \frac{2}{3} k_2 \left( \frac{c^2 R}{GM} \right)^5 \quad \text{where } k_2 \text{ is the quadrupole Love number.}$$

Even more useful is the mass-weighted tidal deformability, which applies to unequal-mass binaries too:

$$\tilde{\Lambda} = \frac{16}{13} \frac{(m_1 + 12m_2)m_1^4 \Lambda_1 + (m_2 + 12m_1)m_2^4 \Lambda_2}{(m_1 + m_2)^5}$$

Yet another equivalent parameter used is the tidal polarisability parameter for a binary  $\kappa_2^T$ . Bernuzzi et al. PRL115, 2015, showed that the dimensionless gravitational-wave frequency depends on the stellar EoS, binary mass and mass ratio, only through this tidal coupling constants  $\kappa_2^T$ .

$$\kappa_2^T = 3 \left( \frac{q^4}{(1+q)^5} \Lambda_1 + \frac{q}{(1+q)^5} \Lambda_2 \right)$$

$$q = m_1/m_2$$

# Tidal deformations

- Several studies made clear that it is possible to measure the deformability (and so radius) of compact stars from BNS inspirals.
- **With increasing amounts of details and physical/detector effects taken into account, these works predicted that radius would be measured to 10% or better with one or few observations.**
- Read et al. PRD88, 2013, quantified data-analysis estimates of the measurability of matter effects in neutron-star binaries on the basis of numerical-relativity simulations.
- We analysed numerical waveforms produced with different numerical setups and by different groups and combined with the detector noise curve.
- We used an extended set of equations of state, modelled as piecewise polytropes.
- We analysed the measurability of neutron-star radius  $R$  and of the tidal deformability parameter  $\Lambda$ .

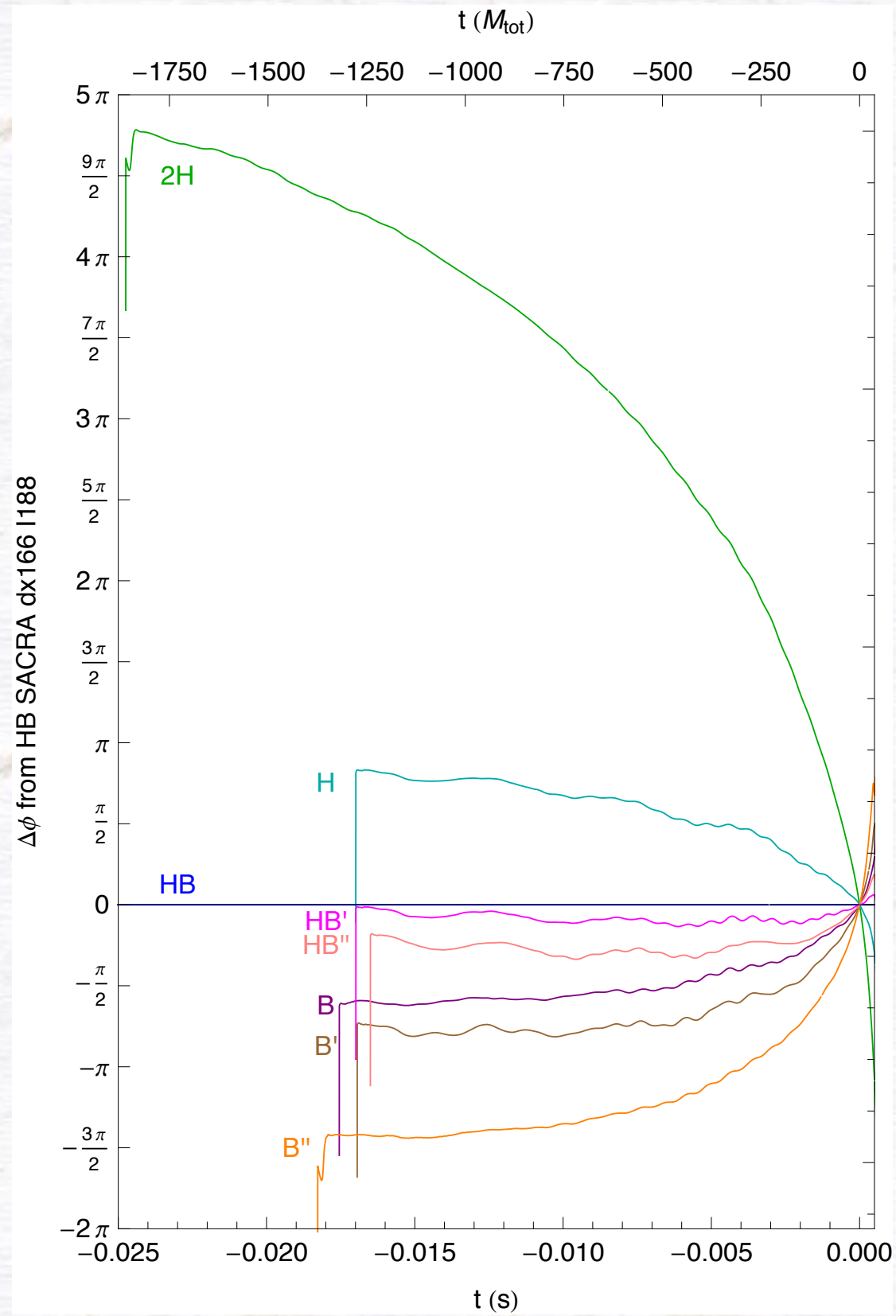
# Choice of EoS

In this work we chose two density intervals and the EoS were labelled by Read et al. PRD79, 2009, as 2H, H, HB, B..., namely with the hardness/blackness scale used for graphite pencils.

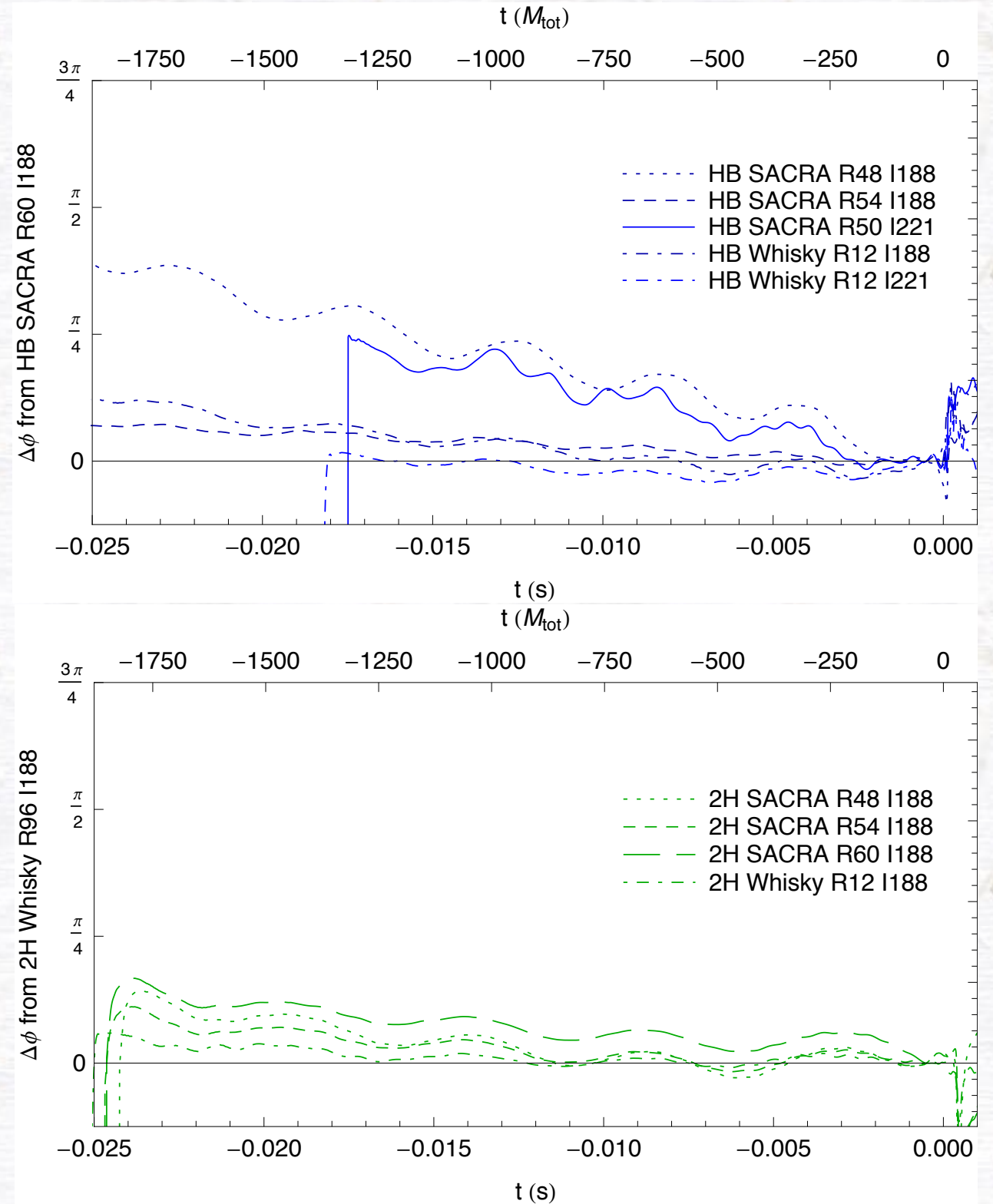
Model	$\log_{10} p_1$ [dyn cm <sup>-2</sup> ]	$R$ [km]	$GM/c^2 R$	$M_{\max}[M_{\odot}]$
2H	34.90	15.2	0.13	2.83
H	34.50	12.3	0.16	2.25
HB	34.40	11.6	0.17	2.12
B	34.30	10.9	0.18	2.00
2B	34.10	9.7	0.21	1.78

# Numerical differences vs. different EoS

## Physical differences



## Numerical differences



# Measurability estimates

- In order to estimate our ability to measure the radius of the neutron star  $R$  or its tidal deformability  $\Lambda^{1/5}$  for a detected signal, we create a one-parameter family of waveforms,  $h(p)$ , where  $p$  is the EoS-dependent parameter of interest (either  $R$  or  $\Lambda^{1/5}$ ) and compare the detected signal to the members of this family in order to determine the value of the parameter that produces the best match.
- Such comparisons are based on a noise-weighted inner product. This inner product of two waveforms  $h_1$  and  $h_2$ , for a detector with noise spectrum  $S_h(f)$ , is defined by

$$\langle h_1 | h_2 \rangle = 4\Re \int_0^\infty \frac{\tilde{h}_1(f) \tilde{h}_2^*(f)}{S_h(f)} df$$

# Distinguishable waveforms

- Two waveforms,  $\mathbf{h}(\mathbf{p}_1)$  and  $\mathbf{h}(\mathbf{p}_2)$  are said to be distinguishable if the quantity

$$\rho_{\text{diff}} = \sqrt{\langle h(p_1) - h(p_2) | h(p_1) - h(p_2) \rangle}$$

has a value larger than one.

- The importance of numerical effects is estimated by the variance in  $\rho_{\text{diff}}$  between two EoS from differing choices of representative numerical waveform.

Advanced LIGO high-power detuned

EOS	H	HB	B
2H	$2.162 \pm 0.030$	$2.210 \pm 0.036$	$2.234 \pm 0.035$
H	-	$0.896 \pm 0.099$	$1.0452 \pm 0.087$
HB	-	-	$0.580 \pm 0.168$

Einstein Telescope configuration D

EOS	H	HB	B
2H	$20.352 \pm 0.314$	$20.739 \pm 0.369$	$20.890 \pm 0.360$
H	-	$7.740 \pm 0.914$	$9.130 \pm 0.866$
HB	-	-	$5.095 \pm 1.490$

# Estimation of errors

There will be statistical and systematic errors on the measure of  $\mathbf{p}$ :

- $\delta p_{\text{stat}}$ : due to random detector noise errors
- $\delta p_{\text{syst}}$ : due to errors (uncertainties) in numerical simulations

$$\delta p_{\text{stat}} \simeq \frac{|p_1 - p_2|}{\sqrt{\langle h(p_1) - h(p_2) | h(p_1) - h(p_2) \rangle}}$$

$$\delta p_{\text{syst}} \simeq (p_1 - p_2) \frac{\langle h(p_1) - g(p_1) | h(p_1) - h(p_2) \rangle}{\langle h(p_1) - h(p_2) | h(p_1) - h(p_2) \rangle}$$

Here  $\mathbf{g}$  is the reference (best resolved) waveform and  $\mathbf{h}$  is the waveform obtained with other numerical settings.

# Estimation of errors

Waveform 1	Waveform 2	$\bar{R}$	$\delta R_{\text{stat}}$ $\times (D_{\text{eff}}/100 \text{ Mpc})$	$\delta R_{\text{syst}}$	$\bar{\Lambda}^{1/5}$	$\delta(\Lambda^{1/5})_{\text{stat}}$ $\times (D_{\text{eff}}/100 \text{ Mpc})$	$\delta(\Lambda^{1/5})_{\text{syst}}$
EOS 2H to EOS H ( $\Delta R = 2.95 \text{ km}$ , $\Delta\Lambda^{1/5} = 0.555$ )							
2H Whisky R142 I188	H SACRA R54 I221	13.75 km	$\pm 1.39 \text{ km}$		2.08	$\pm 0.26$	
(2H SACRA R286 I188)				+0.003 km			+0.000
(2H SACRA R255 I188)				+0.024 km			+0.004
(2H Whisky R177 I188)				+0.004 km			+0.000
	(H SACRA R275 I221)			+0.029 km			+0.006
EOS H to EOS HB ( $\Delta R = 0.669 \text{ km}$ , $\Delta\Lambda^{1/5} = 0.126$ )							
H SACRA R221 I221	HB Whisky R177 I188	11.94 km	$\pm 0.87 \text{ km}$		1.74	$\pm 0.16$	
(H SACRA R239 I221)				+0.060 km			+0.011
	(HB SACRA R209 I188)			-0.043 km			-0.008
	(HB SACRA R188 I188)			-0.051 km			-0.01
	(HB SACRA R226 I221)			+0.066 km			+0.012
	(HB Whisky R177 I221)			-0.033 km			-0.006
EOS HB to EOS B ( $\Delta R = 0.645 \text{ km}$ , $\Delta\Lambda^{1/5} = 0.123$ )							
HB Whisky R177 I188	B SACRA R177 I221	11.28 km	$\pm 0.77 \text{ km}$		1.61	$\pm 0.15$	
(HB SACRA R209 I188)				-0.106 km			-0.020
(HB SACRA R188 I188)				-0.221 km			-0.042
(HB SACRA R226 I221)				+0.055 km			+0.011
(HB Whisky R177 I221)				-0.162 km			-0.031
	(B SACRA R212 I221)			+0.348 km			+0.066
	(B SACRA R197 I221)			+0.115 km			+0.022
	(B Whisky R177 I221)			+0.268 km			+0.051

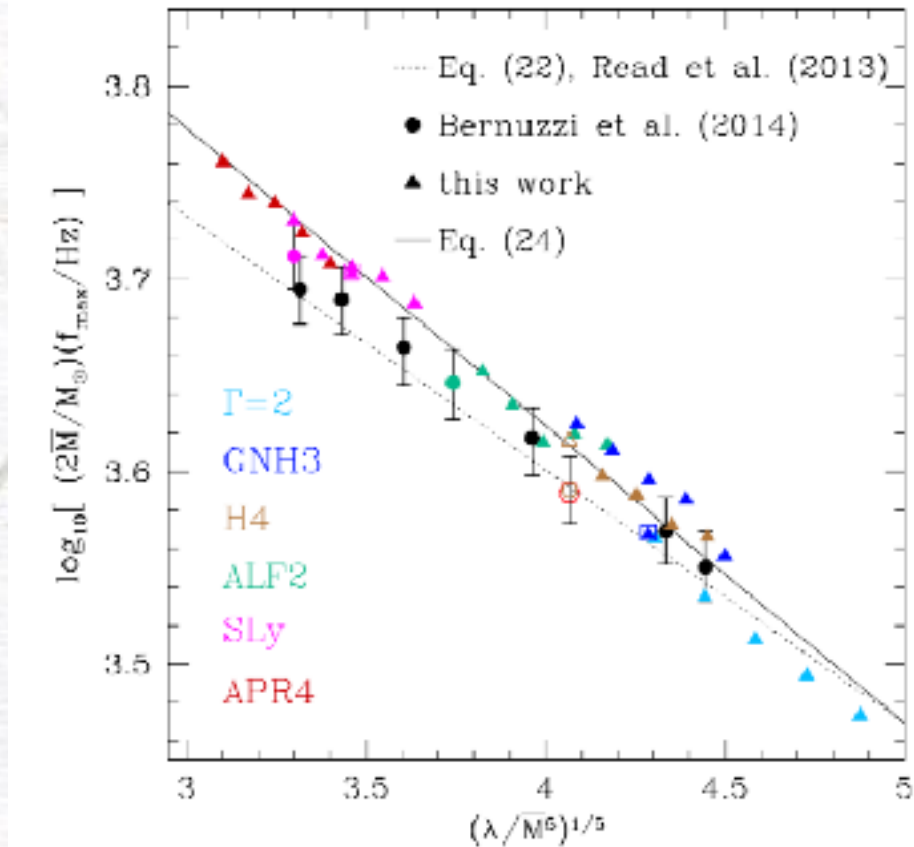
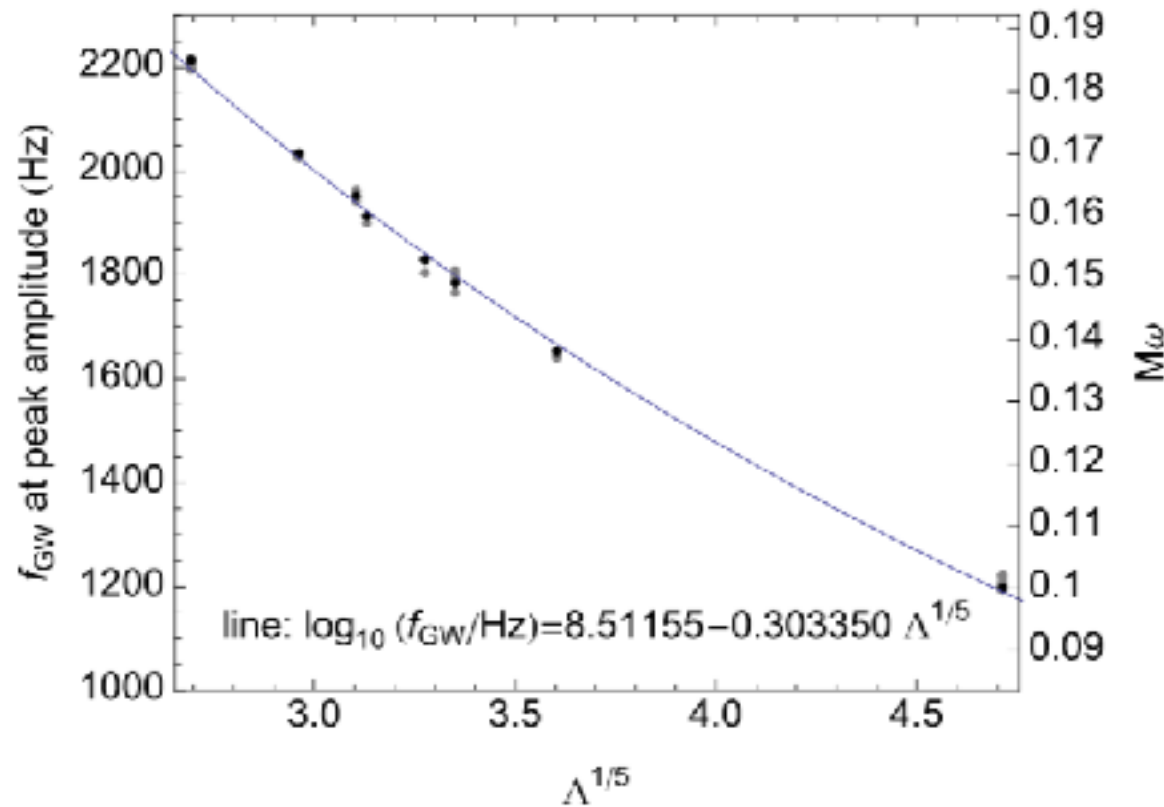
# Hybrid waveforms

- Hybrid waveforms are a match between the numerical waveforms and some approximant (PN+LO+NLO Taylor T4 model for Read et al.)
- Only a portion of the waveform is matched, and the length and time of the matching window is varied to explore the sensitivity of the results to hybridization.
- The variation of the match region for hybrid construction between early and late in the numerical waveforms gives a systematic error of 5%.
- Calculating the systematic differences by changing the numerical waveform used, for a fixed hybrid construction method and PN model (so for a fixed EoS), gives a systematic error  $\delta\Lambda^{1/5} / \Lambda^{1/5} \approx 3\%$ .
- The significance of higher-order PN tidal terms is estimated by dropping the NLO tidal contribution. This has little effect on the estimates, giving a systematic error of  $\approx 1\%$ .

# Hybrid waveforms

- Hybrid waveforms were then noticeably improved by using
  - better numerical-relativity simulations:
    - higher resolution
    - smaller initial orbital eccentricity
  - better approximants:
    - resummed Post-Newtonian (PN) expressions (Dietrich et al. PRD96, 2017)
    - tidal effective one body (TEOB) (Kawaguchi et al. PRD 97, 2018)
  - either in the time domain (Dietrich et al. PRD96, 2017) or directly in the frequency domain (Kawaguchi et al. PRD 97, 2018)
- Through comparison with numerical relativity simulations, these works obtained tidal corrections to the gravitational-wave phase and amplitude that can be efficiently used in data analysis.
- Kawaguchi et al. PRD 97, 2018 found **the statistical error for the measurement of the mass-weighted tidal deformability is more than 6 times larger than the systematic error** for signal-to-noise ratio 50. They also showed that the statistical error for the measurement of the mass-weighted tidal deformability is larger than the variation of the mass-weighted tidal deformability with respect to the mass ratio even for the signal-to-noise ratio 100.

# Tidal deformations



- Read et al. PRD88, 2013, were also the first to find a universal relation between the frequency of the merger and the tidal deformability  $\Lambda$  of the neutron stars in an equal-mass binary.
- The frequency of the merger is defined as the instantaneous gravitational-wave frequency at the time when the amplitude reaches its first peak.
- The relation is said to be universal because it is valid for all the EoSs tried, which include a large range of compactness.
- The relation was later confirmed by more advanced works, like Bernuzzi et al. PRL112, 2014, PRL115, 2015, Takami et al. PRD91, 2015.

# Tidal deformations

- Later, it was confirmed with more sophisticated statistical analyses that for neutron-star binaries with individual masses of  $1.4 M_{\odot}$ , the dimensionless tidal deformability  $\Lambda$  could be determined with about 10% accuracy by combining information from about 20–100 sources, depending on assumptions about the BNS population parameters (in particular, assuming nonzero spins for the initial neutron stars shifts the necessary number of sources to higher values) [Del Pozzo et al. PRL11, 2013; Wade et al. PRD89, 2014; Bernuzzi et al. PRD 89, 2014; Lackey Wade PRD91, 2015; Agathos et al. PRD92, 2015]
- Del Pozzo et al. PRL111, 2013, did the first fully Bayesian analysis in a realistic data setting, finding that only a few tens of detections will be required to arrive at strong constraints.
- Lackey Wade PRD91, 2014 and Agathos et al PRD 92, 2015, took into account tidal effects, quadrupole monopole effects and possible early termination of inspiral GW because of finite size of stars.

# Tidal deformations

- Hotokezaka et al PRD93, 2016, have quantitatively improved the computations and estimations of Read et al. PRD88, 2013, in two principal directions.
- First, they employed new numerical-relativity simulations of irrotational binaries with longer inspirals (i.e. 14–16 orbits) and higher accuracy both in the initial-data setup (i.e. residual eccentricity of  $\sim 10^{-3}$ ).
- Second, they included lower frequencies down to 30 Hz in the analysis, to which ground-based detectors like Advanced LIGO are more sensitive; they also adopted additional EoSs.
- Results were very similar to those of Read et al. PRD88, 2013, namely that deformability  $\Lambda$  and radius can be determined to about 10% accuracy for sources at 200 Mpc
- This is because their improvements drew the detectability in opposite directions: increasing the frequency range increases detectability, while better numerical-relativity simulations apparently show smaller tidal effects and so decrease the detectability.
- They conclude that if the EoS of neutron stars is stiff (with a radius around 13 km), it could be pinned down by measurements of the radii obtained with this method, but if the EoS of neutron stars is soft (smaller radii), a single EoS cannot be identified with this method (unless the signal is very strong, in case the source is very close).

Studying the compact-star EoS through  
gravitational waves from BNS systems  
**after the merger**

# After the merger

- Post merger **observations**
  - would probe densities higher than typical densities in merging stars
  - would also probe effects of temperature
  - may emit in GWs more energy than in the inspiral (if no prompt collapse)
  - but since frequencies are higher, their signal-to-noise ratio in current and projected detectors is smaller than in the inspiral
  - they are probably only marginally measurable by detectors like Advanced LIGO. Third-generation detectors, such as ET and CE, are needed
- Numerical **simulations** of the post-merger phase
  - are very difficult because of strong shocks, turbulence, magnetic fields, instabilities, viscosity and other microphysical effects
  - currently cannot reliably determine the phase of post-merger oscillations, but only the frequencies.
- The main peak frequencies of the post-merger spectrum strongly correlate with properties (radius at a fiducial mass, compactness, etc.) of a zero-temperature spherical equilibrium star in an EoS-independent way.

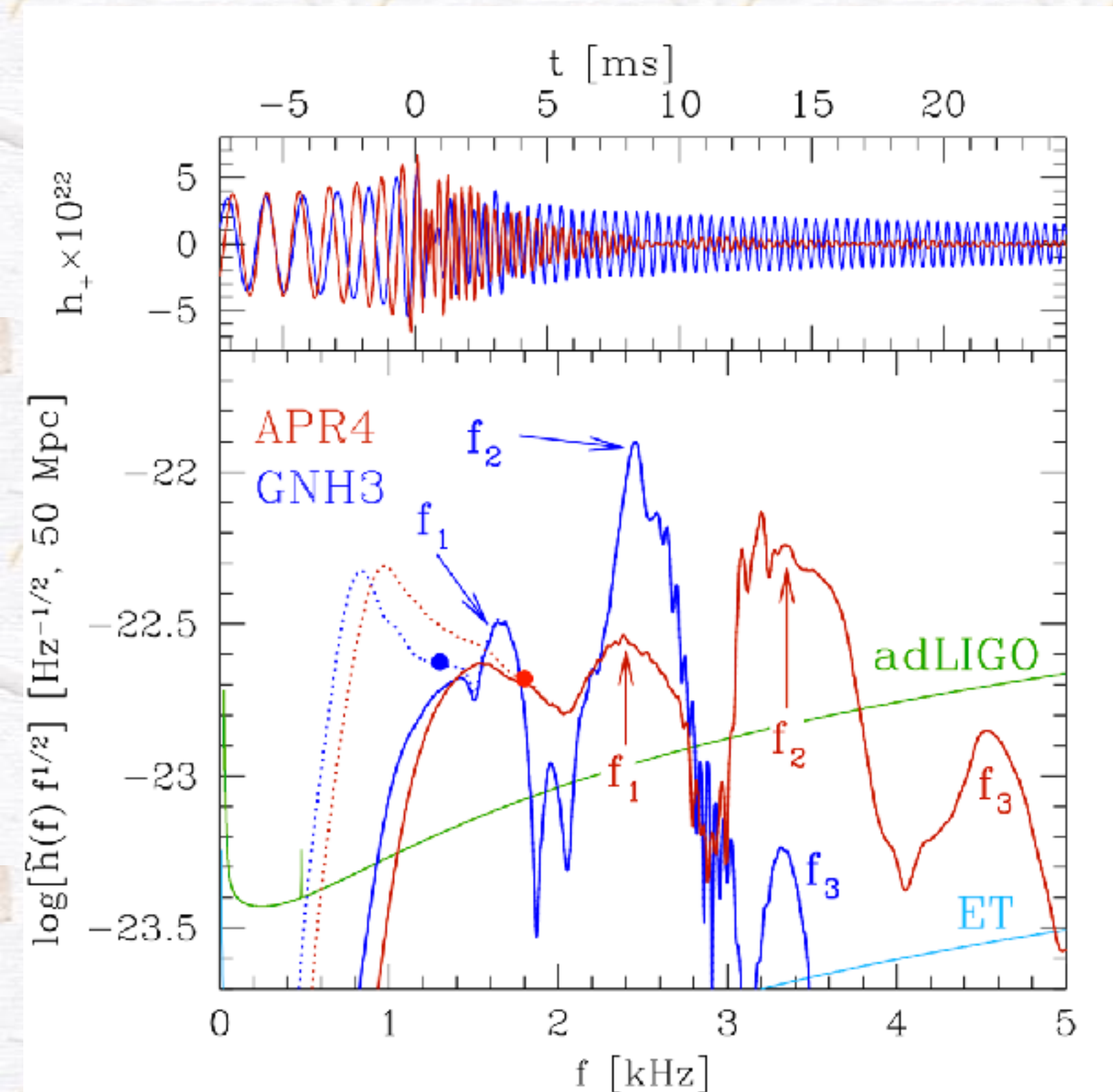
# After the merger

- First attempt by Hotokezaka et al. PRD88, 2013: They decomposed the merger and post-merger gravitational-wave emission into four different parts:
  - (i) a peak in frequency and amplitude soon after the merger starts;
  - (ii) a decrease in amplitude during the merger and a new increase when the compact star forms;
  - (iii) a damped oscillation of the frequency during the compact star phase lasting for several oscillation periods and eventually settling to an approximately constant value (although a long-term secular change associated with the change of the state of the HMNSs is always present);
  - (iv) a final decrease in the amplitude during the HMNS phase, which is either monotonical or with modulations.

Based on this, they found an optimal 13-parameter fitting function, using which it may be possible to constrain the neutron-star radius with errors of about 1 km.

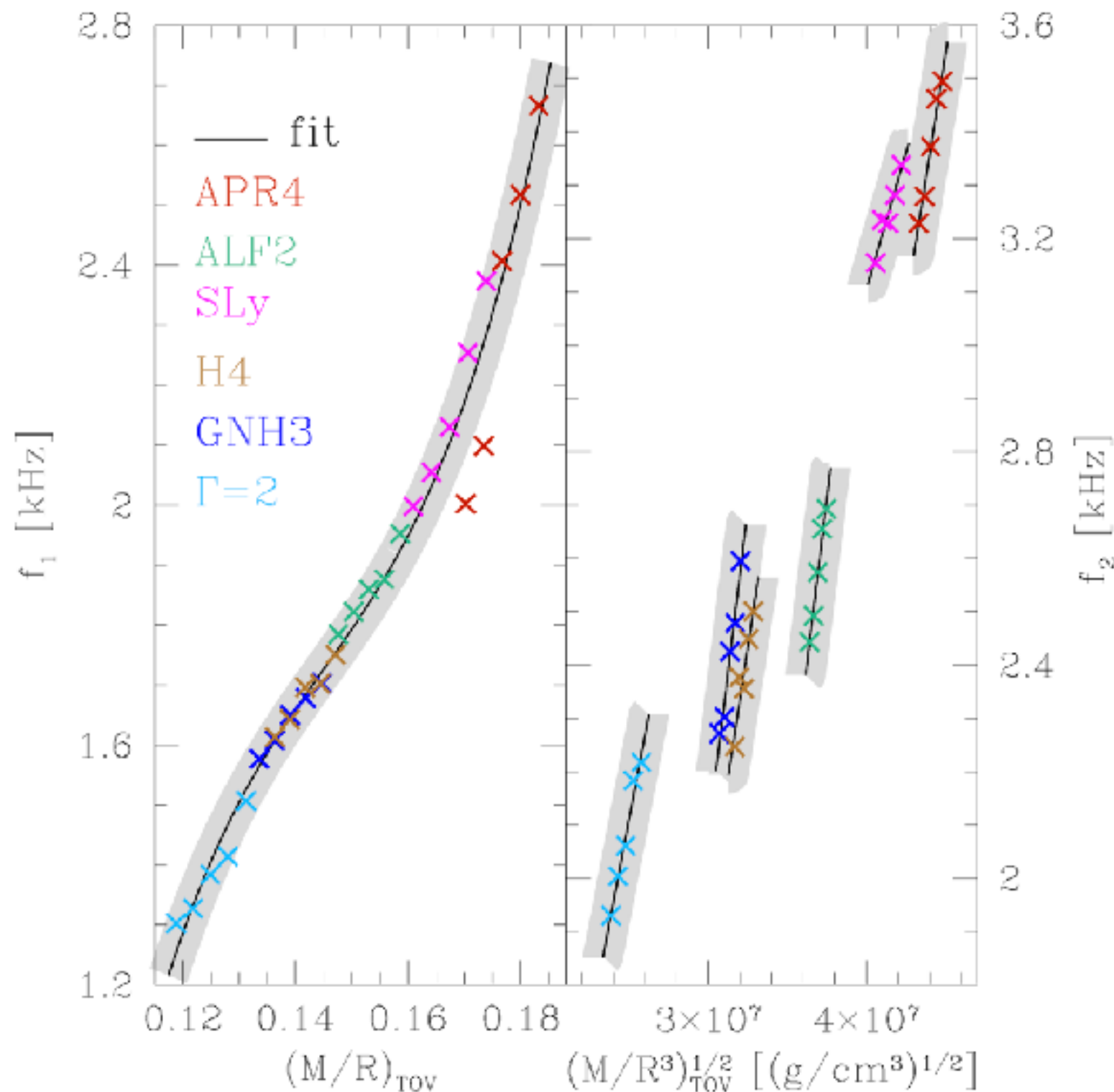
- The first to propose relations between single peak frequencies and stellar properties (mass, radius, compactness and so EoS) were Bauswein Janka PRL108, 2012; Bauswein et al. PRD86, 2012; PRL11, 2013; PRD90, 2014 (with their conformally flat SPH code).
- Subsequent analyses were performed by a number of groups with general-relativistic codes Takami et al. PRL113, 2014; PRD91, 2015; Dietrich et al, PRD91, 2015; Foucart et al. PRD93, 2016; De Pietri et al. PRD93, 2016; Maione et al PRD93, 2016; Rezzolla Takami PRD93, 2016, which confirmed that the conformally flat approximation employed by Bauswein and collaborators provided a rather accurate estimate of the largest peak frequencies in the PSDs.

# Peaks in the merger and post-merger spectra



- Peaks are clearly identifiable in the spectra for each EoS.
- $f_1$  is related to the merger.
- $f_2$  is related to the oscillations of the HMNS.
- $f_3$  has not been well interpreted yet.

# Correlations between peaks and initial stellar properties



- We found correlations between several quantities, the most important of which is the correlation f1 - compactness

- because it seems universal, namely data for all EoSs are well fitted by a single polynomial (cubic).

- This gives a relation:

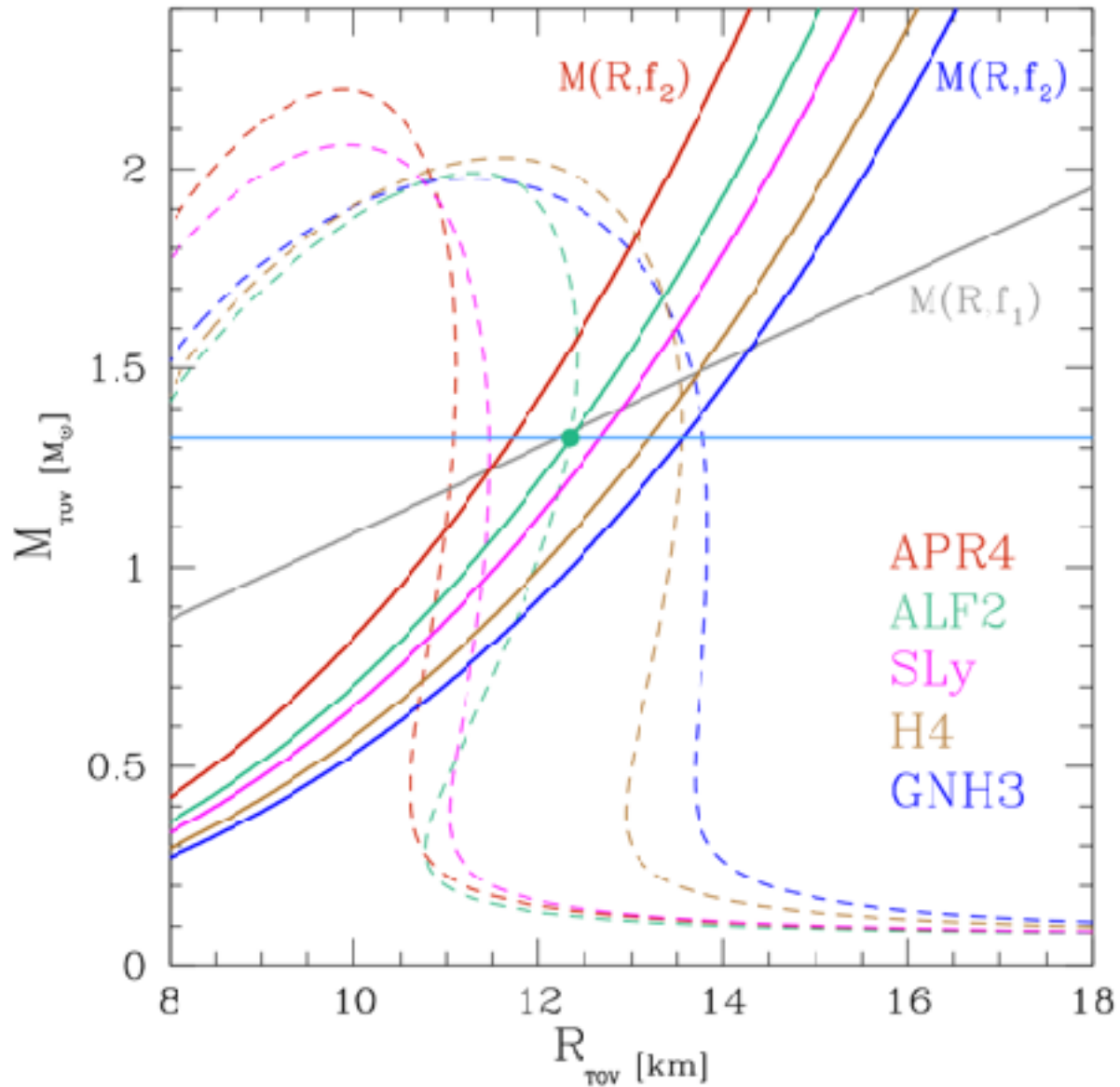
$$\mathbf{M}=\mathbf{M}(f_1, \mathbf{R})$$

- $f_2$  seems not universal: a good fit for each EoS separately only.

- This gives relations

$$\mathbf{M}=\mathbf{M}(f_2, \mathbf{R}, \text{EoS})$$

# Example



- Dashed lines: equilibrium curves of isolated non rotating stars
- Grey:  $M = M(f_1, R)$
- This is not enough, so use:  
 **$M = M(f_2, R, \text{EoS})$**
- If this is not yet enough (like in this example), then use the  $M$  measured in the inspiral

# Remarks

- In principle, the procedure can work with just one detection, in practice uncertainties may make it difficult, but the possible degeneracies mentioned above could be removed with a few positive detections, which would tend to favour one EoS over the others.
- If only the  $f_2$  frequency is measured, the approach discussed above can still be used as long as the mass is known.
- Our considerations result from simulating (equal- or unequal-mass) irrotational binaries.
- Bernuzzi et al PRD89, 2014, found that the main peak frequency  $f_2$  is influenced by the initial state of rotation, especially for very rapidly rotating neutron stars.
- Since the  $f_1$  peak is produced soon after the merger, it should not be affected significantly by magnetic fields and radiative effects, whose modifications emerge on much larger timescales.

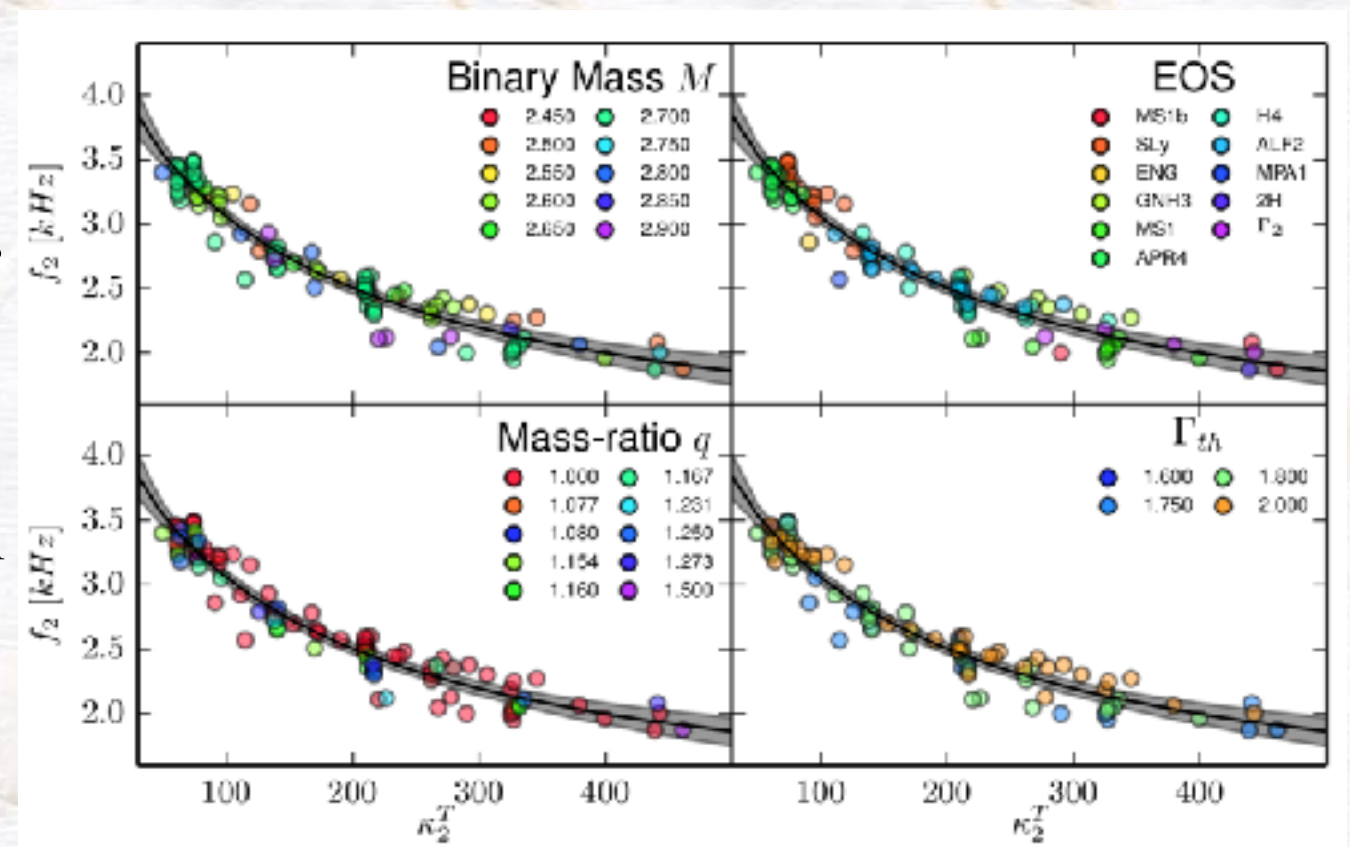
# Remarks

- GW measurements at the expected frequencies and amplitudes are very difficult, and limited to sources within  $\sim 30$  Mpc for second generation detectors, as shown by Clark et al. PRD91, 2014; CQG33, 2016, Yang et al. PRD97, 2018, via a large-scale Monte Carlo study and improved data-analysis techniques .
- Clark et al. CQG33, 2016, also showed that the error in the estimate of the neutron-star radius would be of the order of 400 m in aLIGO.
- Yang et al. PRD97, 2018, proposed methods that stack the post-merger signal from multiple binary neutron star observations to boost the post-merger detection probability.
- They find that, after one year of operation of Cosmic Explorer, the peak frequency can be measured to a statistical error of  $\sim 4\text{--}20$  Hz for certain EoS, corresponding to a radius measurement to within  $\sim 15\text{--}56$  m, a fractional relative error  $\sim 4\%$ .
- They show that errors in the universal relations between post-merger oscillation frequency and binary total mass and in the template construction dominate over the statistical error.
- Detectability of individual events could potentially improve if one considers all components/peaks that arise in the post-merger waveform, and not only the dominant peak.
- Post-merger frequencies evolve in time, albeit only slightly. Hence, the spectral properties of the gravitational-wave signal can only be asserted reliably when the signal-to-noise ratio is sufficiently strong so that even these changes in time can be measured in the evolution of the PSDs.
- In light of these considerations, the prospects for high-frequency searches for the post-merger signal are limited to rare nearby events.

# After the merger

- An interesting extension of our work has been done by [Bernuzzi et al. PRL115, 2015](#).
- They observed that the coupling constant  $\kappa_2^T$  that parametrizes the late-inspiral of tidally interacting binaries, can also be used to determine the main features of the post-merger GW spectrum, instead of the tidal deformability parameter  $\Lambda$ .
- The relation  $f_2(\kappa_2^T)$  depends very weakly on the binary total mass, mass-ratio, and EoS. However, there is dependence on stellar spins.

- Physical explanation. At fixed separation, the tidal interaction is more attractive for larger values of  $\kappa_2^T$ . Larger  $\kappa_2^T$  binaries merge at lower frequencies (larger radii). As a consequence, the remnants of larger  $\kappa_2^T$  binaries are less bound and have larger angular momentum support at formation. The  $f_2$  frequency seems mainly determined by these initial conditions, other physical effects having negligible influence on the frequency value.

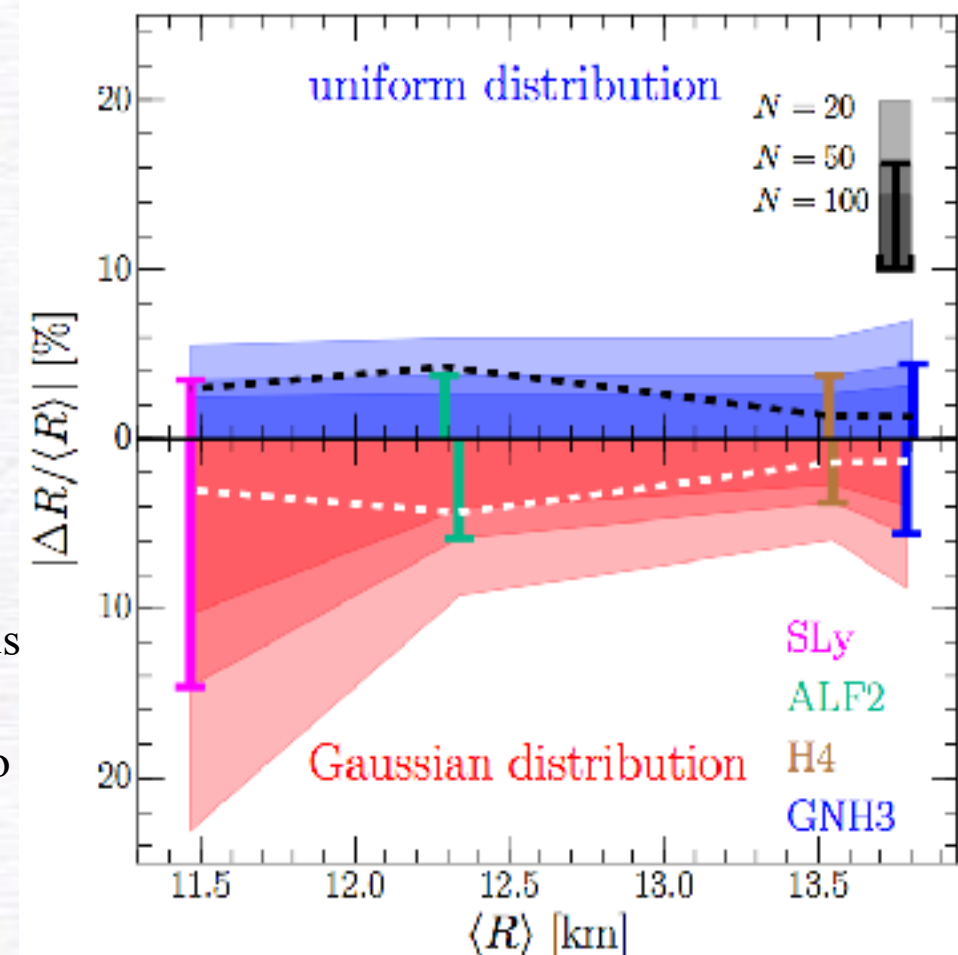


# Combining pre- and post-merger waves

## •Summary

- The tidal deformation method allows determination of the stellar radius to  $\approx 10\%$  with a single close source ( $< 100\text{Mpc}$ ) or with  $\approx 20$  fainter sources ( $\approx 50$  for initially spinning stars in the binary; Bernuzzi et al. PRD 89, 2014; Agathos et al. PRD 92, 2015)
- The post-merger oscillation frequency method allows for a detection horizon of only about 13–27 Mpc for optimally oriented sources and so to an event rate of  $\sim 0.01\text{--}0.1\text{ yr}^{-1}$  (depending also on detection techniques).
- By combing the two methods in a more sophisticated and complete analysis based on Monte-Carlo simulations to estimate the mean population radius, Bose et al. PRL120, 2018, found improved estimates:
  - Error in radius 2-5% for stiff EoSs and 7-12% for soft EoSs
  - As number of observations increases, statistical error decreases and systematic error from simulations will become dominant

*Figure.* Estimated relative error in the radius measured, at 90% confidence level, versus the average population radius for different EoSs and  $N = 20, 50, 100$  (different shadings) BNSs distributed uniformly in a volume between 100 and 300 Mpc. The two panels refer to binaries whose distribution in mass in the range  $[1.2, 1.38]\text{ M}$  is either uniform (top) or Gaussian (bottom). Shown with dashed lines are the errors from the Fisher-matrix analysis for  $N=50$ .



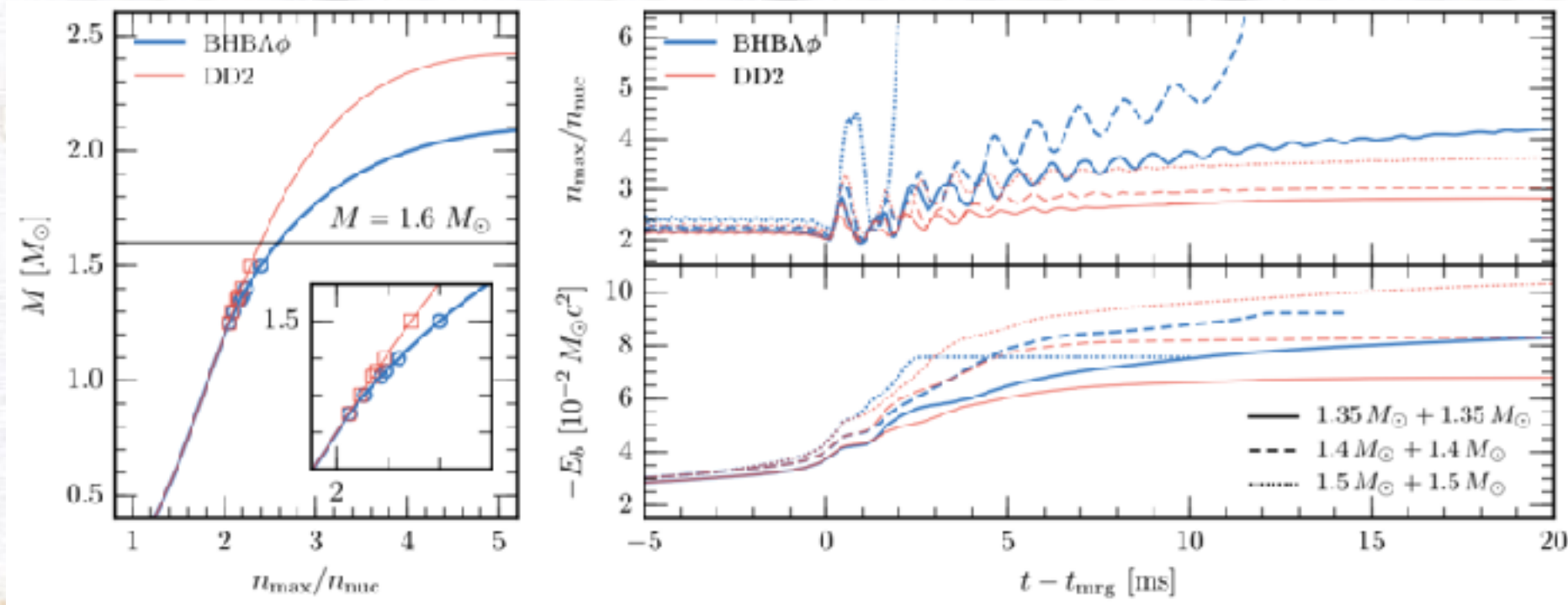
# After the merger

- Another method was proposed that relies less on numerical-relativity simulations (Chatziioannou et al. PRD96, 2017).
- Use Bayesian data analysis algorithm, BAYESWAVE and employ its morphology-independent approach to reconstruct the post-merger GW signal through a sum of appropriate basis functions.
- BAYESWAVE uses wavelets to reconstruct the signal and does not overfit the data.
- BAYESWAVE is capable of reconstructing the dominant features of the injected signal, including the dominant post-merger frequency, with an overlap of above 90% for post-merger SNRs above  $\sim 5$ .
- Can measure  $f_{\text{peak}}$  to within about 36 (27) [45] Hz at the 90% credible level for a stiff (moderate) [soft] EoS at a post-merger SNR of 5 and so set bounds on the NS radius obtained by the post-merger signal of order 100 m for a signal emitted at 20 Mpc (similar to existing phenomenological models, but obtained here without suffering from systematic uncertainties from over-relying on uncertain numerical simulations).
- They use an empirical relation from numerical relativity to relate radius and  $f_{\text{peak}}$ ; the systematic uncertainty of such a “universal” relation is always larger than their statistical measurement error. Namely, their error on the radius is dominated by the scatter in the “universal” relation, rather than the statistical error of the reconstruction.

# Distinguishability of phase transitions

- Radice et al. ApJLett842, 2017, proposed a proof of principle of how GW from post-mergers can probe phase transitions at extreme densities.
- Phase transitions and extra degrees of freedom can emerge at densities beyond those reached during the inspiral, and typically result in a softening of the EoS.
- They adopt two temperature and composition-dependent EoSs for this work: the DD2 EoS and the BHB $\Lambda\phi$  EoS. Probably generalisable to all EoSs for which a high-density phase transition would be allowed by current constraints, in particular, the existence of 2 solar-mass NSs. The reason being that the main effects are a consequence of the EoS softening at densities larger than  $2.2 n_{\text{nuc}}$  and are not specific to the appearance of  $\Lambda$ -particles.

# Distinguishability of phase transitions



Radice et al. ApJLett842, 2017

- Negligible differences in the inspiral, because the EoSs agree until  $n=2.5 n_{\text{nuc}}$ .
- The formation of hyperons in the interface layer between the NSs during merger results in a catastrophic loss of pressure support, which leads to a more violent merger.
- After merger, the BHBA $\phi$  remnants are characterized by a progressive increase of the hyperon fraction in their cores, which causes their rapid contraction, while the DD2 remnants remain more extended.
- The waveforms start to be distinguishable only after merger, with the BHBA $\phi$  binaries becoming significantly louder in GWs after merger, with different amplitude modulation and phase evolution. Their peak frequencies are very similar.
- Adv. LIGO could rule out one of the two possibilities with a single merger at a distance of up to  $\sim 20$  Mpc, depending on the total mass of the binary. This increases up to  $\sim 200$  Mpc with ET.

# Semi-raw data from GW170817

Abbot et al.  
PRL **119**, 161101 (2017)

PHYSICAL REVIEW LETTERS

week ending  
20 OCTOBER 2017

TABLE I. Source properties for GW170817: we give ranges encompassing the 90% credible intervals for different assumptions of the waveform model to bound systematic uncertainty. The mass values are quoted in the frame of the source, accounting for uncertainty in the source redshift.

	Low-spin priors ( $ \chi  \leq 0.05$ )	High-spin priors ( $ \chi  \leq 0.89$ )
Primary mass $m_1$	$1.36\text{--}1.60 M_\odot$	$1.36\text{--}2.26 M_\odot$
Secondary mass $m_2$	$1.17\text{--}1.36 M_\odot$	$0.86\text{--}1.36 M_\odot$
Chirp mass $\mathcal{M}$	$1.188^{+0.004}_{-0.002} M_\odot$	$1.188^{+0.004}_{-0.002} M_\odot$
Mass ratio $m_2/m_1$	$0.7\text{--}1.0$	$0.4\text{--}1.0$
Total mass $m_{\text{tot}}$	$2.74^{+0.04}_{-0.01} M_\odot$	$2.82^{+0.47}_{-0.09} M_\odot$
Radiated energy $E_{\text{rad}}$	$> 0.025 M_\odot c^2$	$> 0.025 M_\odot c^2$
Luminosity distance $D_L$	$40^{+8}_{-14}$ Mpc	$40^{+8}_{-14}$ Mpc
Viewing angle $\Theta$	$\leq 55^\circ$	$\leq 56^\circ$
Using NGC 4993 location	$\leq 28^\circ$	$\leq 28^\circ$
Combined dimensionless tidal deformability $\tilde{\Lambda}$	$\leq 800$	$\leq 700$
Dimensionless tidal deformability $\Lambda(1.4M_\odot)$	$\leq 800$	$\leq 1400$

0.1% error

1% error

While the chirp mass is well constrained, estimates of the component masses are affected by the degeneracy between mass ratio and the aligned spin components.

Constraints imposed by or deduced from  
GW170817  
on the compact-star EoS

# Constraints from GW170817

- Estimates and constraints on EoSs (compact-star radius) on the basis of
  - a) The upper bound on the tidal deformability in GW170817
  - b) The upper bound for the maximum mass for a non-rotating compact star deduced in various ways from GW170817
  - c) The lower bound for the maximum mass for a non-rotating compact star from other observations  $M_{\text{max}} > 2.01 M_{\odot}$
- c) requires stiff enough EoS ( $R_{1.4}=R(1.4M_{\odot}) > 11.1 \text{ km}$ ) while a) and b) require soft enough EoS ( $R_{1.4} < 13.4 \text{ km}$ )

# Constraints from GW170817

smooth EoS, no phase transitions

- Some works studied how their favourite EoS (families) fit with the constraints from GW170817
- The two most recent articles on this line are
  - Lim Holt arXiv1803.02803
  - Most et al. arXiv1803.00549
- They have some small differences and share common results
- Generalise efforts of previous works that had used a specific set of EoSs
- Assume a smooth EoS (no phase transitions)
- Parameterise (in different ways) a very large range of physically plausible EoS for compact stars
- Obtain equilibrium solutions for up to one million different EoS by numerically solving the Tolman-Oppenheimer-Volkoff (TOV) equations

# Constraints from GW170817

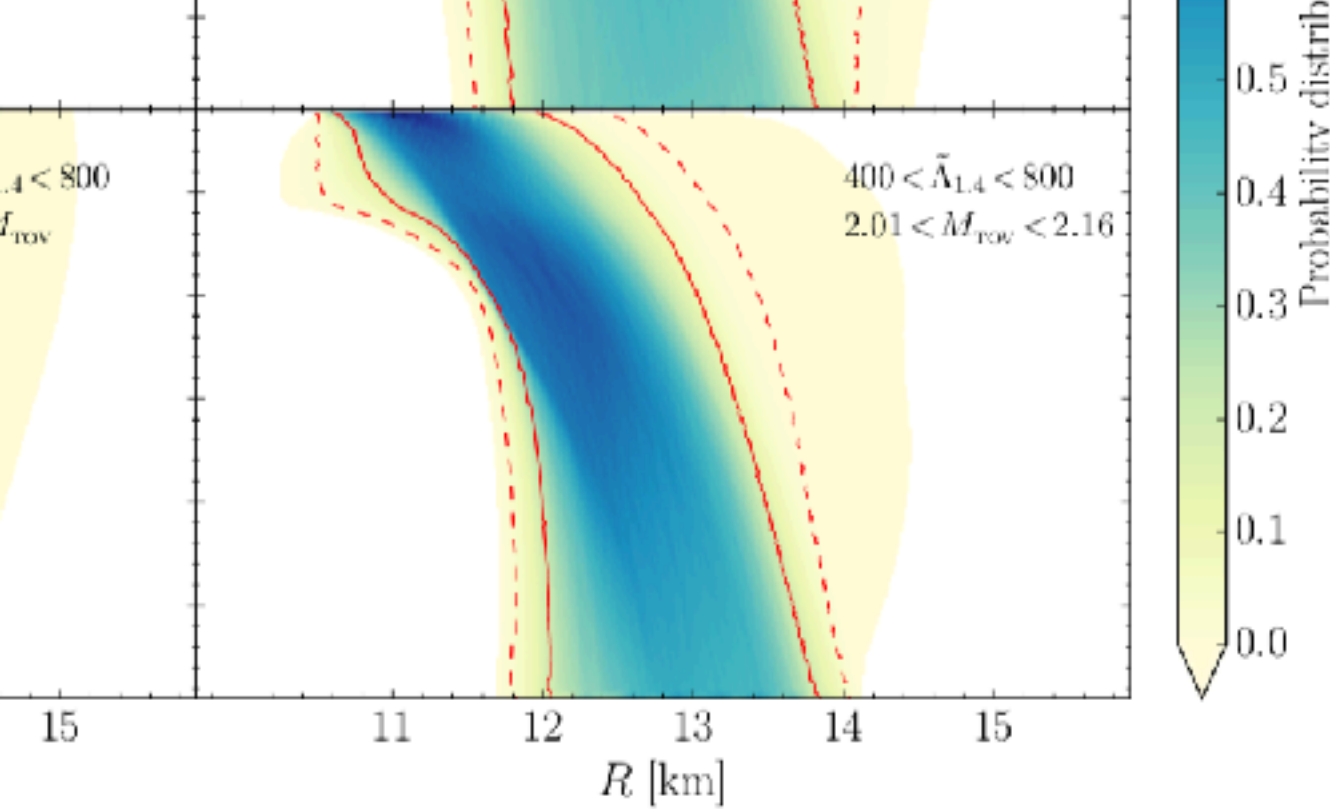
smooth EoS, no phase transitions

- Use a cold EoS constructed by matching the behaviour in the low- and high-density regimes (from the outer crust to the inner core, assuming a composition consisting of protons, neutrons, and electrons), by chiral effective field theory, using piecewise polytropes (details differ in the two works)
- Impose constraints:
  - sound speed is subluminal
  - the tidal deformability  $\Lambda_{1.4}$  from GW170817 is  $< 800$
  - the lower bound on the maximum mass for a non-rotating NS ( $M_{\max} > 2.01$ )
  - the upper bound on the maximum mass for a non-rotating NS ( $M_{\max} < 2.16$ ) (only Most et al. arXiv1803.00549)
- Carry out the first systematic study of the statistical properties of the tidal deformability highlighting that the lower limit for  $\Lambda_{1.4}$  is tightly constrained.

# Constraints from GW170817

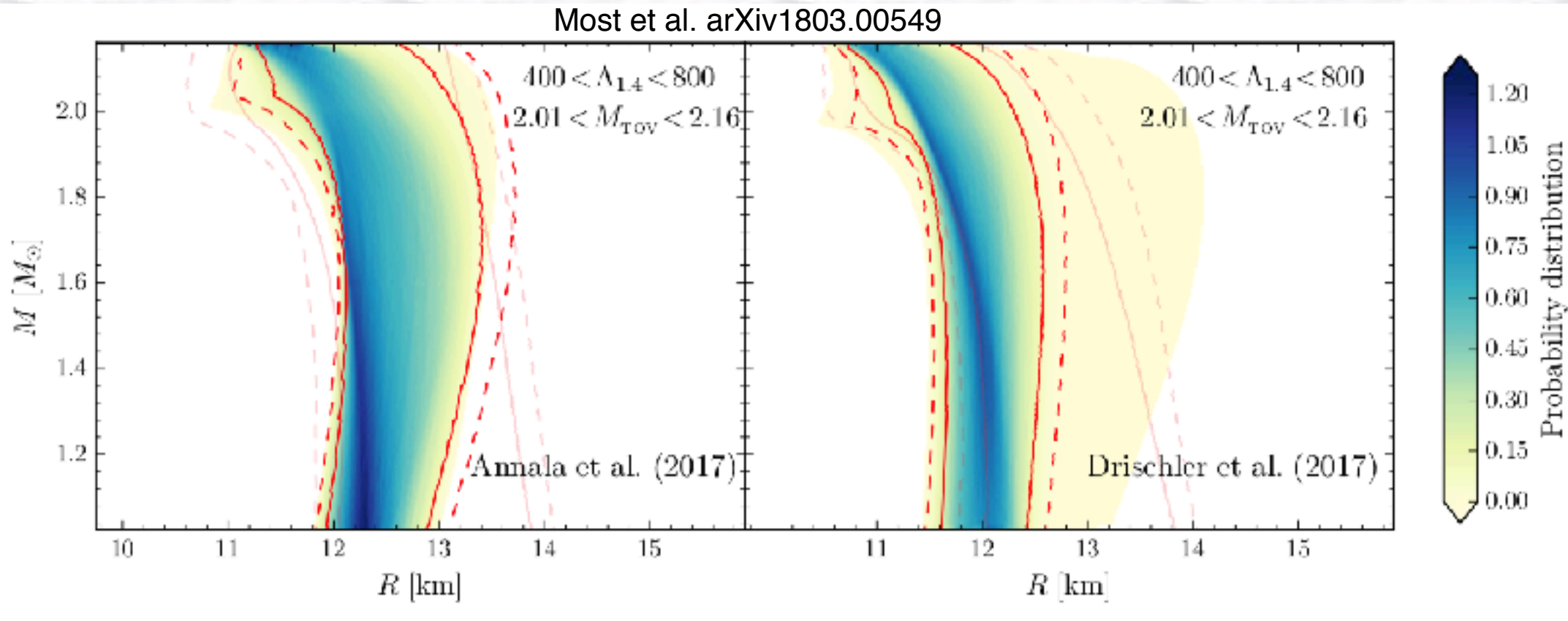
smooth EoS, no phase transitions

Most et al. arXiv1803.00549



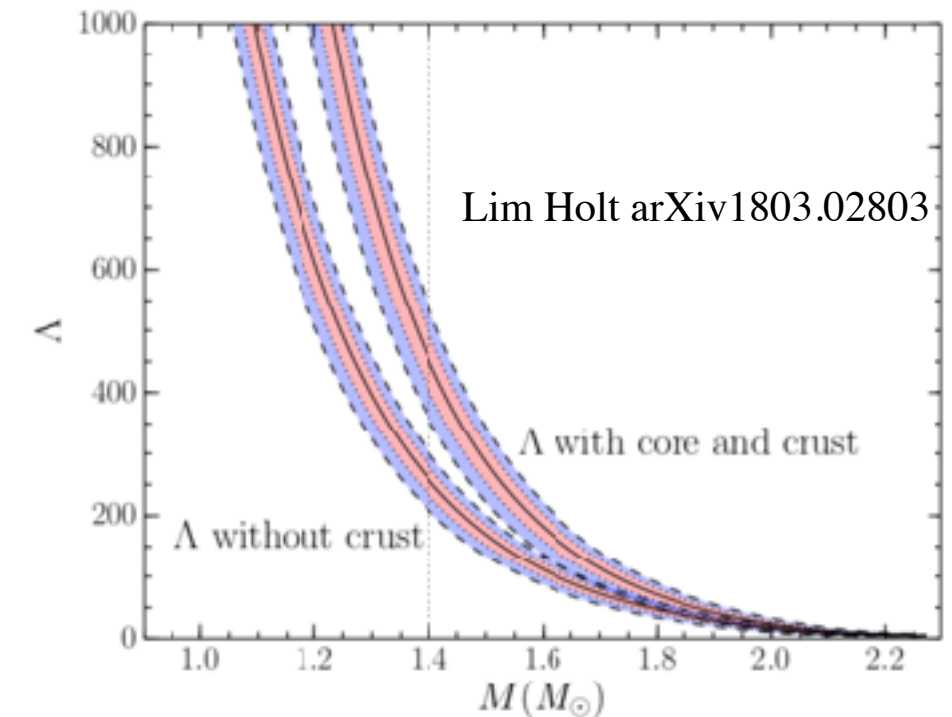
- The bottom-right panel shows the probability distribution when limits are set both on the maximum mass and on the tidal deformability, i.e.,  $2.01 M_{\odot} < M_{\max} < 2.16 M_{\odot}$  and  $400 < \Lambda_{1.4} < 800$ .
- The distribution is peaked around the small-radii end of the range.
- In this way, they constrain  $12.00 < R_{1.4} < 13.45$  at a  $2\text{-}\sigma$  confidence level, with a most likely value of  $R_{1.4} = 12.45$ .
- The distributions are very robust upon changes in upper limit of the maximum mass.
- Changing the upper limit of the tidal deformability, e.g., considering  $\Lambda_{1.4} < 700$  does not change the distribution significantly, because the upper limit on the maximum mass effectively removes many of the stiff EoSs that have large values of  $\Lambda_{1.4}$ .
- The smallest dimensionless tidal deformability is  $\Lambda_{1.4} > 375$  at a  $2\text{-}\sigma$  level.

# Constraints from GW170817



This figure shows the impact that different prescriptions on the treatment of the nuclear matter in the outer core may have on the statistical properties of neutron star radii.

As expected, the crust has an important influence on the tidal deformability



# Constraints from GW170817

smooth EoS, no phase transitions

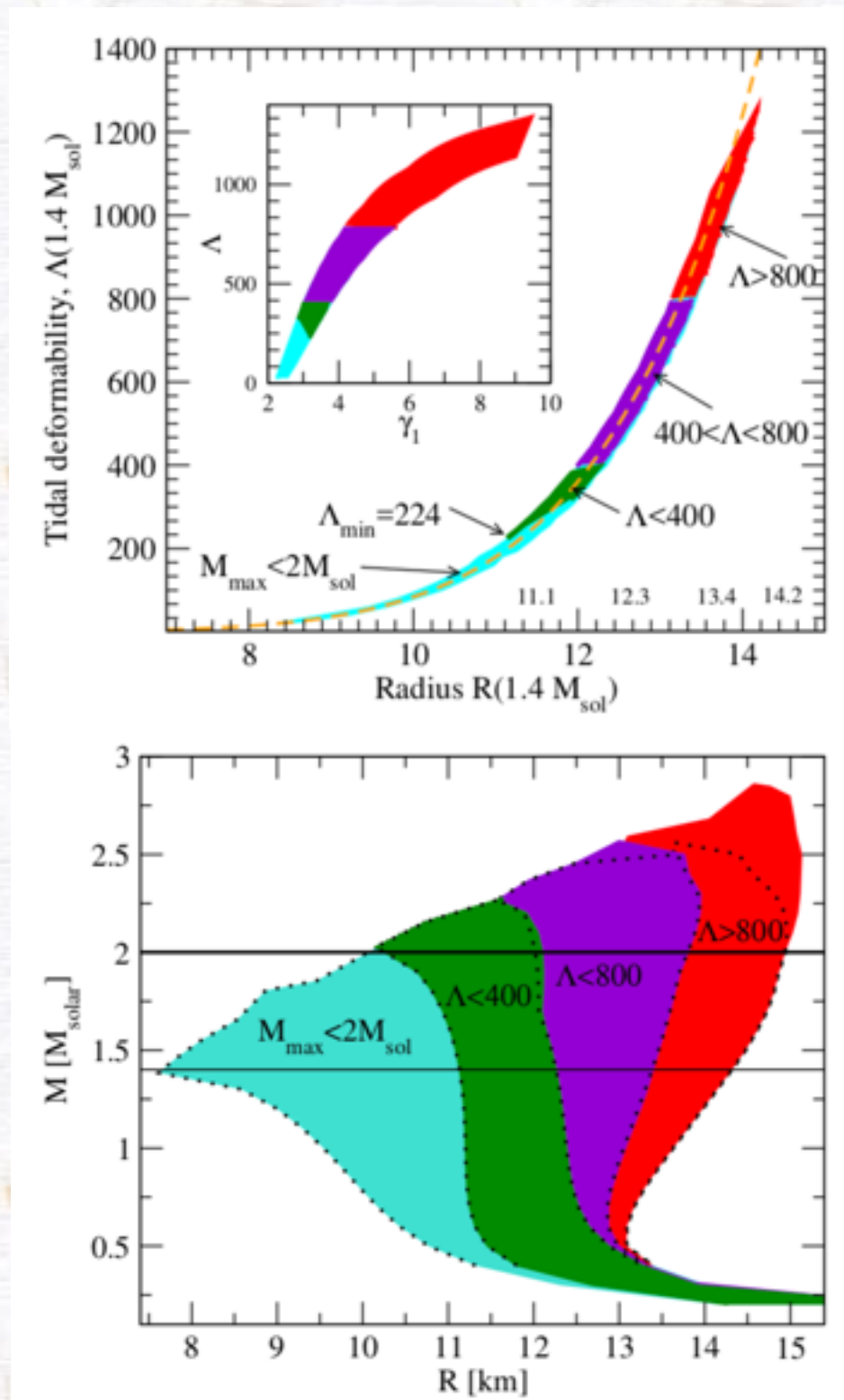
- **Differences in the results** of Lim Holt arXiv1803.0280 and Most et al. arXiv1803.00549
  - Radius at a 2- $\sigma$  confidence level
    - Most et al. arXiv1803.00549:  $12.00 \text{ km} < R_{1.4} < 13.45 \text{ km}$  with a most likely value of 12.45 km
    - Lim Holt arXiv1803.02803:  $11.65 \text{ km} < R_{1.4} < 12.84 \text{ km}$  with a most likely value of 12.3 km
  - There is a systematic difference of about 0.5 km, but the uncertainty band is similar
- **Common results**
  - Lower bounds on the tidal deformability are much more restrictive to our present theories of the dense matter EoS
  - Estimates of the stellar matter properties of the outer core ( $0.08 < n/\text{fm}^{-3} < 0.21$ ) have enormous impact on macroscopic stellar properties, so progress in knowledge/estimates of the outer core is important.
  - These constraints on the radii and deformabilities are based on the assumption of a smooth EoS and would change in the presence of a first-order phase transition.

# Constraints from GW170817

smooth EoS, no phase transitions

Preceding and similar works using a smaller set of EoSs found similar results

- [Annala et al., arXiv1711.02644](#)
  - had considered only very stiff and very soft models, to give limits
  - found  $R_{1.4} < 13.4$  km,
  - minimum dimensionless tidal deformability for the same mass is  $\Lambda_{1.4} > 224$  (from the figure).
  - also found that in the Lambda-Radius relation the widest variation is related to the low-density EoS and so GW observations (tidal deformability) will constrain that part most.
- [Krastev Li, arXiv1801.04620](#) use the momentum-dependent-interaction (MDI) EoSs and examine the effects of the symmetry energy  $E_{\text{sym}}(\rho)$  on the tidal properties of coalescing binary neutron stars, obtaining similar limits.



# Constraints from GW170817

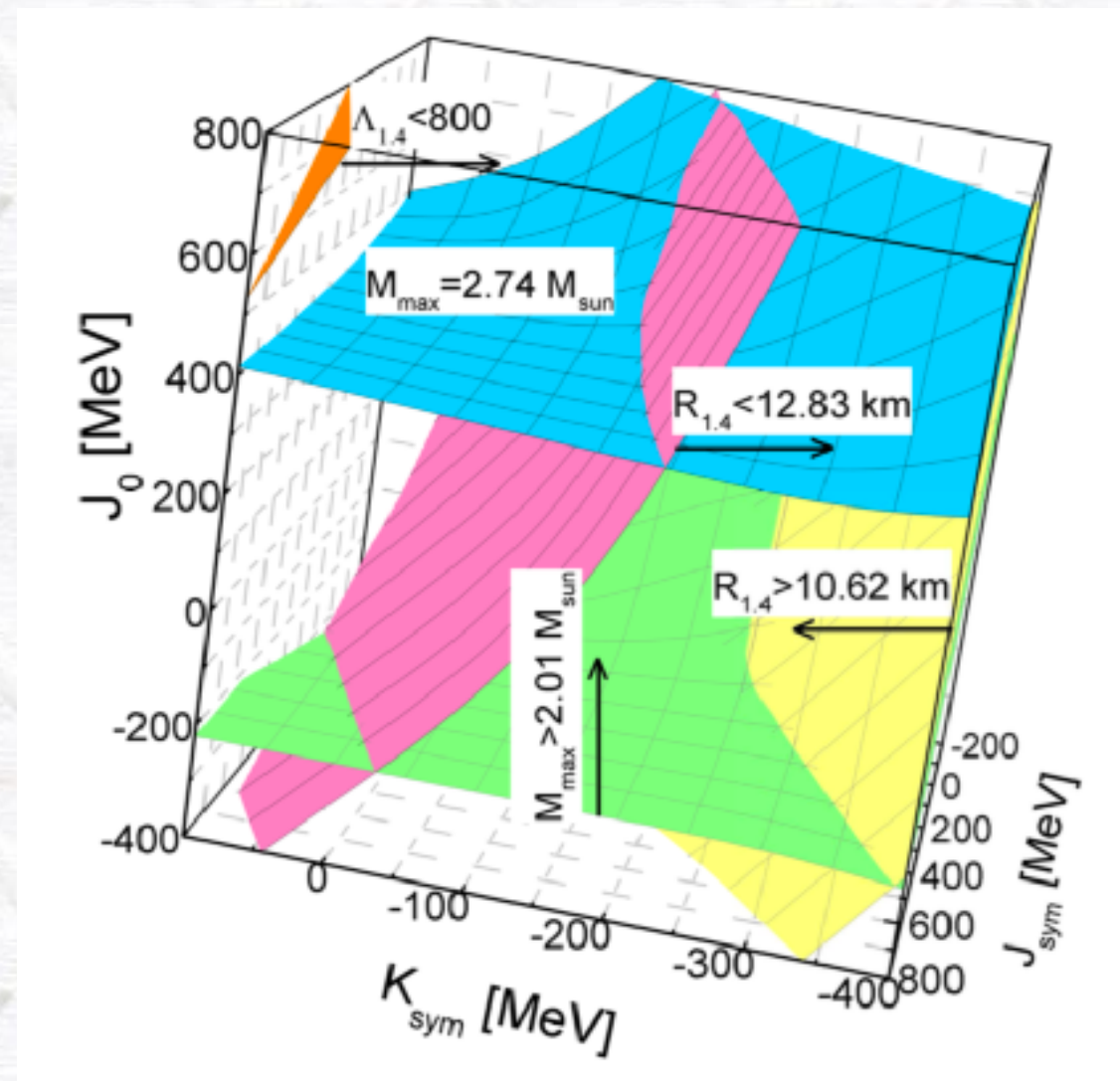
smooth EoS, no phase transitions

- Zhang et al. arXiv1801.06855 studied the specific energy in asymmetric nucleonic matter approximated parabolically in isospin asymmetry in terms of several EoS characteristic parameters:
  - incompressibility  $K_0$  of symmetric nuclear matter (SNM)
  - skewness  $J_0$  of SNM
  - slope  $L$  of symmetry energy at nuclear density  $\rho_0$
  - curvature  $K_{\text{sym}}$  of the symmetry energy
  - skewness  $J_{\text{sym}}$  of the symmetry energy
- Imposed the astrophysical observations of
  - $M_{\text{max}} > 2.01 M_{\odot}$  and  $\Lambda_{1.4} \leq 800$  from GW170817
  - $10.62 < R_{1.4} < 12.83$  km from X-ray binaries
  - constraints from terrestrial nuclear experiments.
- Fixing the  $K_0$ ,  $E_{\text{sym}}(\rho_0)$  and  $L$  at their most probable values mentioned earlier, they explore the intersections of constant surfaces with these astrophysical constraints in the 3-dimensional parameter space of  $K_{\text{sym}}$ ,  $J_{\text{sym}}$  and  $J_0$ .

# Constraints from GW170817

smooth EoS, no phase transitions

- Shown in the figure are the constant surfaces of the NS
    - maximum mass of  $M_{\max} = 2.01 M_{\odot}$  (green),
    - radius of  $R_{1.4} = 12.83$  km (magenta)
    - radius of  $R_{1.4} = 10.62$  km (yellow)
    - upper limit of the dimensionless tidal deformability  $\Lambda_{1.4} = 800$  (orange)
  - the (unlikely) maximum mass for non-rotating compact stars  $M_{\max} = 2.74 M_{\odot}$  (blue) they speculate from the total mass of GW170817.
  - tidal deformability  $\Lambda_{1.4} = 800$  (orange): it locates far outside the constant surface of  $R_{1.4} = 12.83$  km (constraint from X-ray binaries).
- Thus, limits on the high-density EoS parameters from the  $\Lambda_{1.4} \leq 800$  constraint alone are presently much looser than the radius constraint extracted from analysing the X-ray data.



Zhang et al. arXiv1801.06855

# Constraints from GW170817

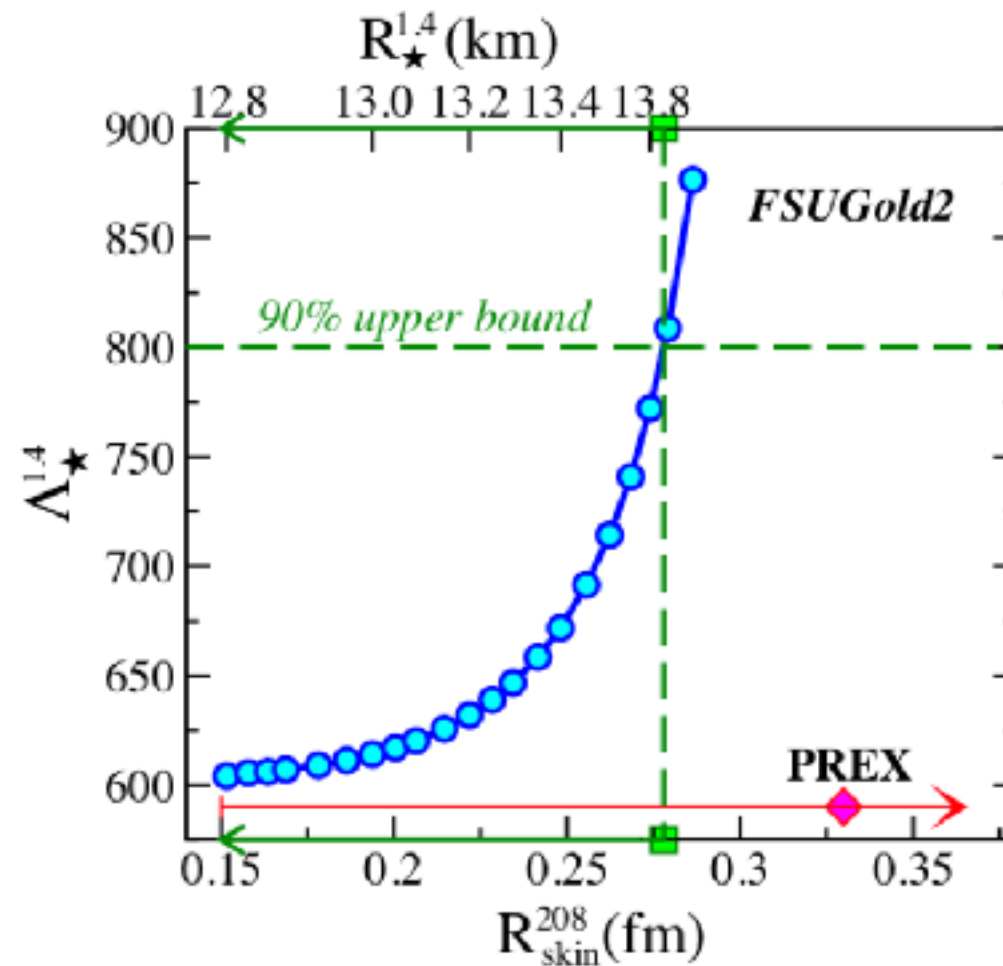
smooth EoS, no phase transitions

Fattoyev et al. arXiv1711.06615 (see also Fattoyev et al. PRC87, 2013; Eur. Phys. J. 50, 2014)

- Compare the tidal deformability observation from GW170817 with data from the PREX experiment on the neutron-skin thickness (the difference between the neutron ( $R_n$ ) and proton ( $R_p$ ) root-mean-square radii) of  $^{208}\text{Pb}$
- Despite a difference in length scales of 19 orders of magnitude, the size of a neutron star and the thickness of the neutron skin are both strongly correlated to the slope  $L$  of the symmetry energy at saturation density and share a common origin: the pressure of neutron-rich matter
- Model the EoS using a relativistic mean-field (RMF) approach (FSUGold2 family and ten others)

# Constraints from GW170817

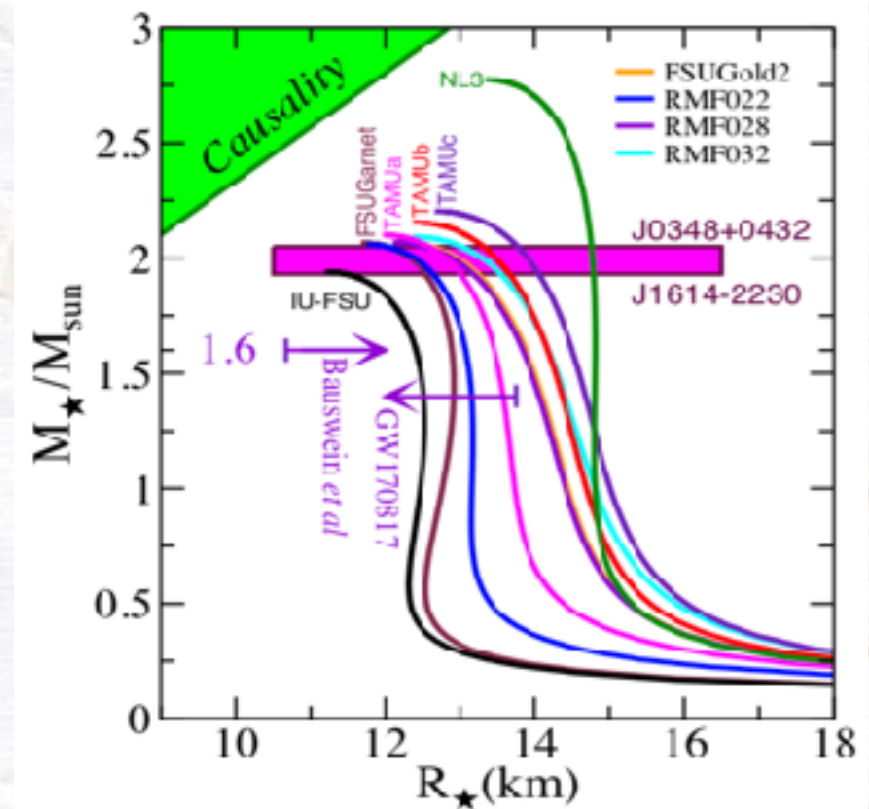
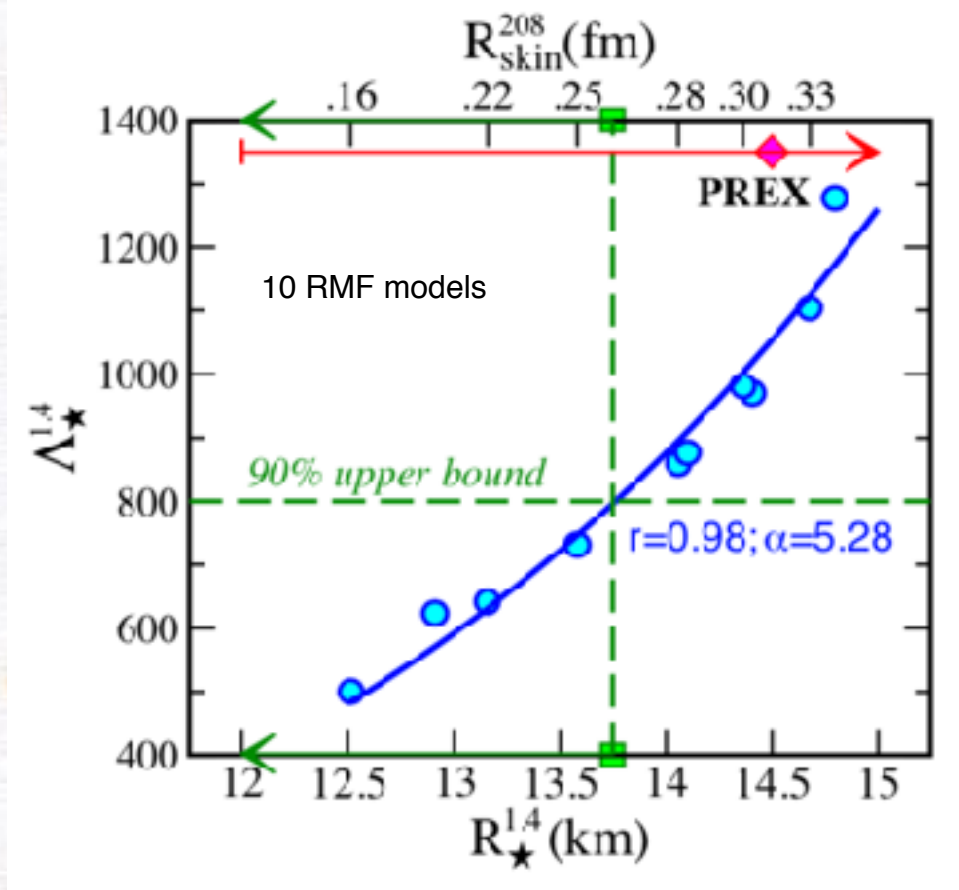
Fattoyev et al. arXiv1711.06615 (see also Fattoyev et al. PRC87, 2013; Eur. Phys. J. 50, 2014)



- The tidal deformability  $\Lambda_{1.4}$  of a  $1.4 M_{\odot}$  neutron star as a function of both neutron-skin thickness  $R^{208}$  and the radius of a  $1.4 M_{\odot}$  neutron star  $R_{1.4}$ .
- $\Lambda_{1.4} \leq 800$  from GW170817 translates into a corresponding upper limit on the radius of a  $1.4 M_{\odot}$  neutron star of  $R_{1.4} \leq 13.9$  km (but no mention is made of the error).
- Adopting the  $\Lambda_{1.4} \leq 800$  limit excludes the  $R^{208} > 0.28$  fm region — suggesting that the neutron-skin thickness of  $^{208}\text{Pb}$  cannot be so large.

# Constraints from GW170817

Fattoyev et al. arXiv1711.06615 (see also Fattoyev et al. PRC87, 2013; Eur. Phys. J. 50, 2014)



- If the large value of  $R^{208}$  is confirmed by the more accurate experiment PREX-II, then this would be in tension with GW170817.
- A thick neutron skin would suggest that the EoS at the typical densities found in atomic nuclei is stiff, while the small neutron-star radii inferred from the BNS merger implies that the EoS at higher densities is soft. The evolution from stiff to soft may be indicative of a phase transition in the interior of neutron stars.
- The lower bound on the neutron-skin thickness of  $^{208}\text{Pb}$  of  $R_{\text{skin}} \approx 0.15$  fm imposed by PREX would indicate that  $R_{1.4} \approx 12.55$  km or  $\Lambda_{1.4} \approx 490$ . Combining observational constraints from the LIGO-Virgo collaboration with laboratory constraints from the PREX collaboration, the tidal deformability of a  $1.4M_{\odot}$  neutron star falls within the range:  $490 < \Lambda_{1.4} < 800$ .

# Constraints from GW170817

## quark stars

- Zhou et al. arXiv1711.04312, making use of the simple but widely-used MIT bag model, describe unpaired strange quark matter (SQM) as a mixture of quarks (u, d, s) and electrons (e), allowing for the transformation due to weak interaction between quarks and leptons.
- Characterize the star properties by the strange quark mass ( $m_s$ ), an effective bag constant ( $B_{\text{eff}}$ ), the perturbative QCD correction ( $a_4$ ), as well as the gap parameter ( $\Delta$ ) when considering quark pairing, and investigate the dependences of the tidal deformability on them.
- Infer that the tidal deformability constraint from GW170817 is compatible with a binary quark star merger.
- Set the lower limit  $\Lambda_{1.4} > 510.1$  for quark stars that are compatible with the  $M_{\text{max}} > 2.01 M_{\odot}$ .
- The tidal deformability is rather insensitive to  $m_s$ ,  $a_4$ ,  $\Delta$ , and mostly depends on  $B_{\text{eff}}$ ; GW170817 constrains it to  $134.1 < (B_{\text{eff}})^{1/4} < 141.4$  MeV.
- Note: The finite surface density of QSs also requires a correction on the surface when calculating the tidal deformability, therefore constraints on NSs according to the observation of GW170817 cannot be simply applied in the scenario of BQS merger.
- However, quark stars are not thought to provide the ejecta necessary to produce the observed macronova emission.

# Constraints from GW170817

phase transitions: hybrid quark stars

- Paschalidis et al. arXiv 1712.00451 were the first to investigate how GW170817 can constrain the properties of hybrid hadron-quark compact stars (HS)
- Constructed hybrid hadron-quark EoSs that:
  - consist of zero-temperature nuclear matter in  $\beta$ -equilibrium with a low-density phase of nucleonic matter and high-density phase of quark matter
  - are supplemented with the low-density EoSs of crustal matter
  - are consistent with the existence of  $2M_{\odot}$  pulsars
  - result in low-mass twins (NSs and HSs having the same mass but different radii) at  $\sim 1.5M_{\odot}$
  - consist of a single-phase quark core enclosed by a hadronic shell with a first-order phase transition at their interface
- The tidal deformation observed from GW170817 is found to be consistent with the coalescence of a binary HS-NS
- Certain hadronic EoSs that do not satisfy the GW170817 constraints on the tidal deformation, become compatible with GW170817 if a first-order phase transition occurs in one of the stars
- Binary HS-NS simulations in full general relativity are necessary for further comparison with BNS
- Note: For NS EoSs the dimensionless tidal deformability can be approximated as linear function of the gravitational mass in the vicinity of  $1.4M_{\odot}$ , but this is not true for hybrid hadron-quark EoSs with low-mass twins. As a result, using this approximation to estimate the tidal deformability of a  $1.4M_{\odot}$  objects should be avoided because it excludes the possibility of testing for HSs.

# Constraints from GW170817

## phase transitions: hybrid quark stars

- Drago et al. ApJLett852, 2018, propose a “two-family” scenario:
  - hadronic stars stable up to  $1.5 - 1.6 M_{\odot}$ ;
  - more massive compact stars are strange quark stars;
  - a transition occurs in finite time during collapse/merger.
- The process of conversion can be divided into two different stages (Drago Pagliara PRC92, 2015):
  - (a) a turbulent combustion, which, in a timescale  $t_{\text{turb}}$  of the order of a few milliseconds, converts most of the star; and
  - (b) a diffusive combustion, which converts the unburnt hadronic layer in a timescale  $t_{\text{diff}}$  of the order of 10 seconds.
- Prompt collapse after a binary merger happens in 1 ms, so for it quark deconfinement is not relevant.
- One-family and two-family scenarios predict different rates for prompt collapses after merger, because the threshold masses allowed for their EoSs are different.
  - one-family:  $M_{\text{threshold}} \approx 2.8 M_{\odot}$  (Bauswein Stergioulas PRD91, 2017, and others) leads to  $P_{\text{prompt}} < 18\%$  (upper limit), by using the mass distribution of Kiziltan et al. ApJ778, 2013;
  - two-family:  $2.52 M_{\odot} < M_{\text{threshold}} \approx 2.72 M_{\odot}$  and  $34\% < P_{\text{prompt}} < 82\%$ , significantly larger than in the case of the one-family scenario.

# Constraints from GW170817

phase transitions: hybrid quark stars

- Drago et al. Universe 4, 2018 (arXiv 1802.02495)
- GW170817 cannot be a binary of hadronic stars (in the two-family scenario), because it would have undergone prompt collapse
- GW170817 cannot be a binary of quark stars, because it would be difficult to explain the macronova which is powered by nuclear radioactive decays
- GW170817 could be a binary of one hadronic and one quark star:
  - the prompt collapse is avoided by the formation of a hypermassive hybrid configuration,
  - whose ejecta may give rise to the macronova
  - the hybrid star configuration predicted by this model can survive as a hypermassive configuration for a time of the order of hundreds of ms.
  - for an asymmetric binary, characterised by  $q = 0.75 - 0.8$ , the predicted tidal deformability of the lightest star (the hadronic one) can reach value of  $\sim 500$

# Constraints from GW170817

strangeon stars = strange-quark-clusters stars

Lai et al. Research in Astronomy and Astrophysics 18, 2018

- Lai and Xu MNRAS Lett. 398, 2009, suggested that quark clustering is possible at the density of a cold compact star and proposed an EoS for them (LX EoS).
- The LX EoS is a stiff EoS with a nonzero surface density.
- The tidal deformability of binary strangeon stars is different from that of binary neutron stars, because a strangeon star is self-bound on the surface by the fundamental strong force while a neutron star by gravity.
- Although the strangeon star EoS is so stiff that the TOV maximum mass would reach  $\sim 3 M_{\odot}$ , the tidal deformability is actually similar to those soft EoS models.
- The tidal deformability of a strangeon star has been estimated to be 381.9, so it is compatible with GW170817.
- The ejecta composed of strangeon nuggets would not lead to r-process nucleosynthesis, but the observed blue component of macronova AT 2017gfo following GW170817 could be powered by the decay of ejected strangeon nuggets, while the late “red component” could be powered by the spin-down of the remnant strangeon star after merging.

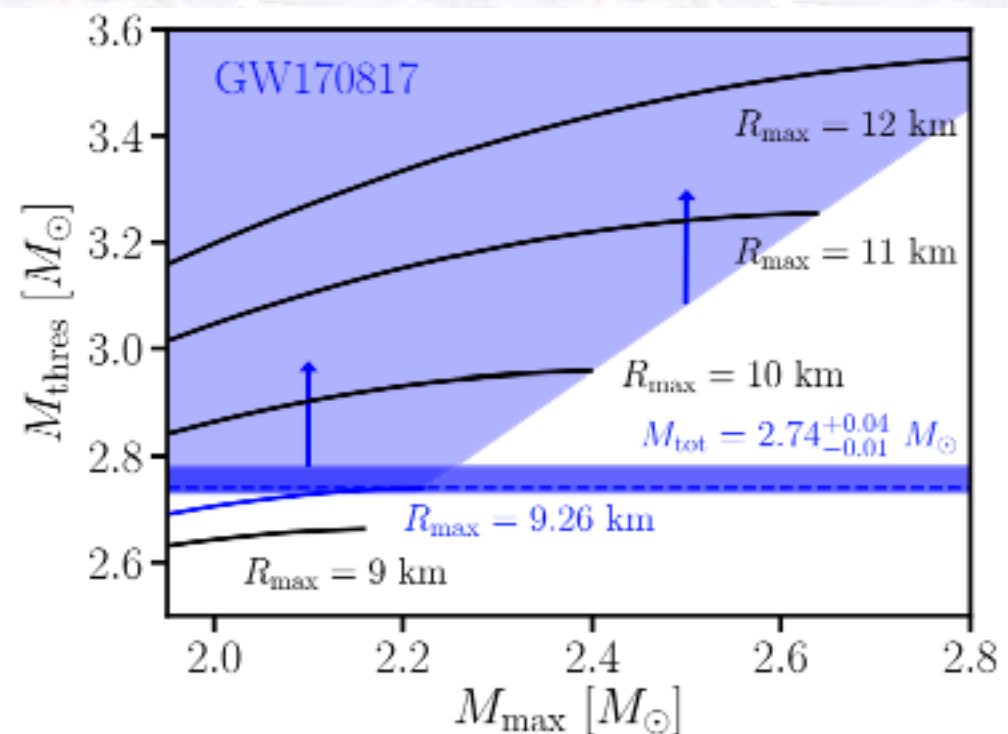
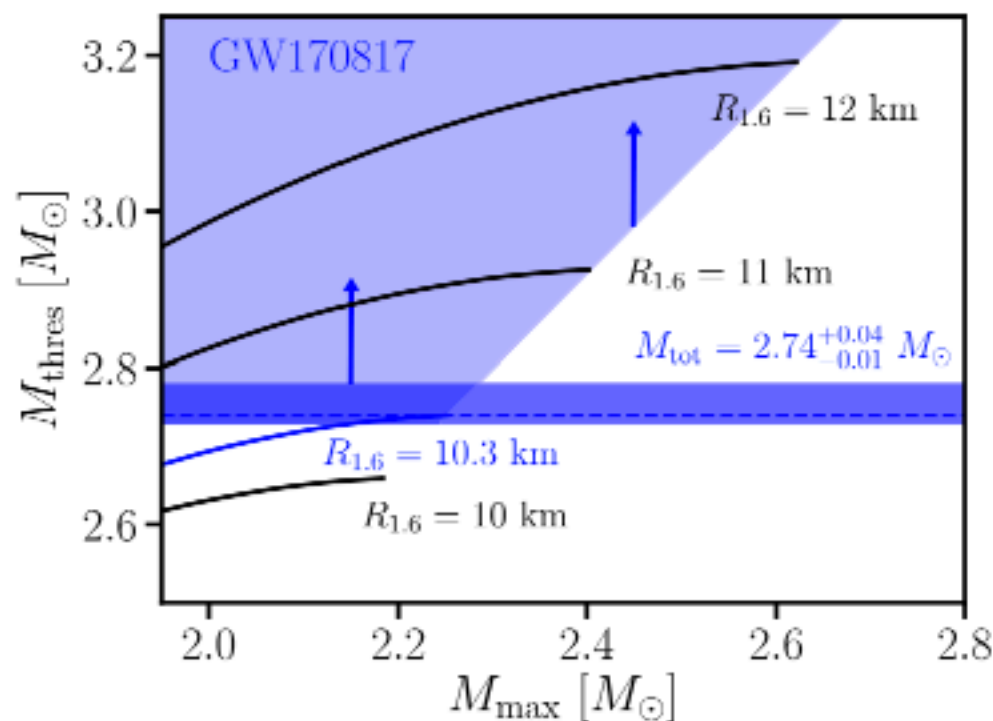
# Constraints from GW170817

Bauswein et al. ApJLett850, 2017, use their empirical relations from simulations between threshold mass for prompt collapse, maximum mass for non rotating star and radius of the star to set constraints on the stellar radius from GW170817.

$$M_{\text{thres}} = \left( -3.606 \frac{GM_{\text{max}}}{c^2 R_{1.6}} + 2.38 \right) \cdot M_{\text{max}}$$

$$M_{\text{thres}} = \left( -3.38 \frac{GM_{\text{max}}}{c^2 R_{\text{max}}} + 2.43 \right) \cdot M_{\text{max}}$$

- GW170817 was not a prompt collapse, so its total mass is a lower bound on the threshold. Compute  $M_{\text{max}}$  and radii.
- Causality imposes an empirical constraint:  $M_{\text{thres}} \geq 1.22 M_{\text{max}}$ .
- $R_{\text{max}} > 9.26 (+0.17; -0.03)$  km.
- $R_{1.6} > 10.30 (+0.15; -0.03)$  km.
- These constraints are particularly robust because they only require a measurement of the chirp mass and a distinction between prompt and delayed collapse of the merger remnant, which may be inferred from the electromagnetic signal or even from the presence/absence of a ringdown gravitational-wave (GW) signal.



# Conclusions

- Of course, intense work is ongoing to interpret GW170817 and future observations also with respect to the ultra-high density EoS
- Current radius estimates from interpretations of GW170817 are within  $\sim 1$  km error band
- In combination to constraints of the maximum mass for non-rotating compact stars, this reduces to a certain amount the space of allowed EoSs
- For future observations,
  - statistical errors are predicted to be more important than systematic errors from numerical simulations in the pre-merger phase
  - systematic errors from numerical simulations are predicted to be more important than statistical errors in the post -merger phase